

UC Berkeley
SEMM Reports Series

Title

Rigid Culverts Under High Fills

Permalink

<https://escholarship.org/uc/item/4rc5w9km>

Author

Brown, Colin

Publication Date

1966-07-01

Return to: SESM Library
543 Davis Hall
Univ. of Calif.
Berkeley, California

REPORT NO.
SESM 66-2 *d*

STRUCTURES AND MATERIALS RESEARCH
DEPARTMENT OF CIVIL ENGINEERING

66-2B

RIGID CULVERTS UNDER HIGH FILLS

TRACTIONS ON THE BARREL
AND IN THE SOIL

BY

COLIN B. BROWN

Final report to the Sponsors: Division of
Highways, Department of Public Works,
State of California, and the
Bureau of Public Roads.

JULY, 1966

COLLEGE OF ENGINEERING
OFFICE OF RESEARCH SERVICES
UNIVERSITY OF CALIFORNIA
BERKELEY CALIFORNIA

DIVISION OF STRUCTURAL ENGINEERING
AND STRUCTURAL MECHANICS
UNIVERSITY OF CALIFORNIA
BERKELEY, CALIFORNIA 94720

Structures and Materials Research
Department of Civil Engineering
Report No. SESM 66-2

RIGID CULVERTS UNDER HIGH FILLS--
TRACTIONS ON THE BARREL AND IN THE SOIL

by

Colin B. Brown

Report to

THE DEPARTMENT OF PUBLIC WORKS
STATE OF CALIFORNIA
Under Standard Service Agreement
No. 13366

College of Engineering
Office of Research Services
University of California
Berkeley, California

July, 1966

Contents

Preface	1
Introduction	2
Part I. Theoretical Considerations	4
1.1 Scope of Theory	4
1.2 Incremental Formulation and Analyses	5
1.3 Formulation of Incremental Problem for Computer Solution	10
1.4 Other Considerations in the Analyses	13
1.5 The Effective Modulus of the Fill	18
1.6 Synthesis	26
Part II. San Luis Reservoir Road Relocation Embankment	26
2.1 General Considerations	26
2.2 Material Properties	26
2.3 Computer Analysis	32
2.4 Instrumentation	34
Part III. Analytical and Design Considerations	51
3.1 Traction on the Barrel	51
3.2 Design Aspects of the Culvert	58
3.3 Fill Pressures	58
3.4 Conclusions	64
References	66
Appendix A	68
Appendix B	69

List of Figures

Fig. 1	Center Line Section of Embankment	6
Fig. 2	Typical Element Arrangement	11
Fig. 3	Typical Influence Density Curve	12
Fig. 4	Rock Boundary Conditions	15
Fig. 5	Inclusion Grading Curve	23
Fig. 6	Step Variation of Modulus with V^S	23
Fig. 7	Bounds on E	31
Fig. 8	Schematic of Embankment	33
Fig. 9	Meter Positions	35
Fig. 10	Stress Variation Across Meter	37
Fig. 11	Meter Conditions in Fill	44
Fig. 12	Meter Stress Distribution	45
Fig. 13	Pressure Plot at Meter Location	49
Fig. 14	Analytical Barrel Pressures	52
Fig. 15	Analytical and Measured Barrel Pressures	53
Fig. 16	Variation of Barrel Pressure with Fill Height	54
Fig. 17	Detail of Fig. 16	55
Fig. 18	Long-term Effect of Hay Rotting	59
Fig. 19	Soil Pressures - Experimental and Analytical Results	60

PREFACE

This work describes a theoretical approach to the statement of loads on buried rigid culverts. The methods are applied to an actual culvert on the San Luis Reservoir road location where extensive instrumentation was installed. Comparisons of results were possible. The report involves statements on effective moduli of soil-rock conglomerates, minimum gage dimensions on soil meters, extensive soil and rock testing, counting of rocks in the conglomerate, computer programming and instrument design. The computer program was developed by Messrs. B. W. Smith and R. Hermann. Mr. W. Mostaghel carried out the material tests and helped with the data reduction. Prof. W. Mitchell advised on the soil tests and Prof. D. Pirtz supervised much of the instrumentation design. The aid of the State Division of Highways is acknowledged for the efficiency with which the rock count was accomplished and the meter results taken and reduced.

INTRODUCTION

The stress distribution in bodies which are built up in an incremental manner has been shown^{1,2} to be dependent upon the construction procedure. Where an embankment is formed with a culvert as an inclusion the effect on the culvert must also be dependent upon the history of the fill sequence. Clearly, as the fill is placed in the region below the crown of the culvert the tendency is to cause the crown to rise and the structure to elongate in that direction. With subsequent fill above the crown the effect is reversed but this motion is resisted by the passive pressure of the side fill. These conclusions would not be evident if the final massless fill with culvert inclusion was considered and the effects of gravity applied to this completed body. Two problems are of importance to the engineer: first, the stresses at critical points in the fill and second, the tractions around the barrel of the culvert. With this information the design of embankment and culvert can be carried out reasonably. Both of these problems are sensitive to the construction procedure and history but proper account of these chronological events is seldom possible in an exact theoretical manner. In this work an approximate treatment is developed which is checked by extensive instrumentation in the fill and around an included reinforced

concrete culvert constructed in the San Luis Reservoir road relocation near Los Banos, California.

This paper is divided into three parts. In Part I the theoretical viewpoint is developed in some generality and this is then specially applied to the particular structure being considered in Part II. The finite element method for plane elasticity problems is used and account taken of the properties of the fill, culvert and foundation material. The fill consists of two definite components, a rock-matrix uncemented conglomerate and an organic material placed over the culvert crown to induce "arching" action. The modulus of the multi-phase conglomerate could not be determined by direct test but theoretical bounds were developed by the methods of Hashin³ and Hashin and Shtrickman⁴.

Part III consists of a discussion of the previous work from the analytical and design viewpoints. This discussion makes use of the results of extensive instrumentation in the fill and in the barrel of the culvert.

PART I

THEORETICAL CONSIDERATIONS

1.1 Scope of the Theory

Although existing work provides clear statements of the general physical and mathematical characteristics of the incremental method, the existing applications are for very simple configurations which can be solved completely in closed form. The more complex geometries encountered in this problem necessitate the reformulation of the incremental problem for approximate solution on the digital computer. The solutions for each layer of added material are obtained by use of the linear theory of elasticity and the subsequent summing of these solutions in the continuing process of superposition involves a process well suited to the computer. The individual incremental solutions are obtained by the finite - element technique, the accuracy of which has been well established by usage and also by theoretical investigations of its manner of bounding the true solution. These considerations of the analytical solution are dealt with first. The second portion considers the material properties to be used in the analysis. The heterogeneous nature of the main fill required that effective elastic properties of the conglomerate be sought rather than gross properties from large scale tests. In this case the inclusions in the matrix were of about 12" diameter and the resulting specimen size for gross tests was impractically large. The theoretical bounds developed for the effective properties require only the matrix and inclusion properties and the numerical distribution of the inclusions.

1.2 Incremental Formulation and Analysis

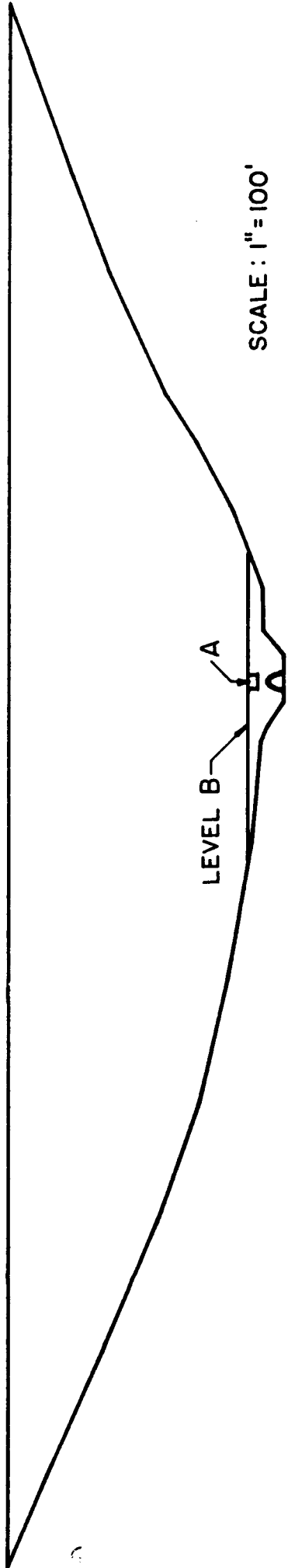
At the end of the last century a remark to G. H. Darwin by Maxwell was confirmed experimentally by the former. This remark concerned the "historical element" affecting the nature of the limiting equilibrium of granular material. By "historical element" is meant that structures of this material put together in different orders and ways exert different forces even though the final appearance is the same. Eighty years later theoretical attempts were made to describe this phenomenon and it was shown that the internal stresses in built-up embankments depend on the construction sequence. Similarly many engineers have realized that the conditions in the barrel of a culvert may vary in a non-monotonic manner as the fill material rises monotonically up the sides and then above the crown of the structure.

Here, we specialize the problem to two dimensions and to the configuration of the embankment near Los Banos in particular. A center line section is shown in Fig. 1. At some time in the construction sequence the upper line of the fill is at A. The effects of a layer of material added to A in the normal manner of construction is to cause displacements and stresses in the existing embankment. If we think of a fixed coordinate system x,y , then the displacements and stress fields are

$$\tilde{U}_i^A = \tilde{U}_i^A(x,y) \quad 1.2.1$$

$$\tilde{\sigma}_{ij}^A = \tilde{\sigma}_{ij}^A(x,y) \quad 1.2.2$$

where i, j may each take values x and y .



SCALE : 1" = 100'

FIG. I

CENTER LINE SECTION OF EMBANKMENT

The addition of a subsequent layer of material at A' makes the layer added at A into an intrinsic part of the embankment and for this new structure the displacement and stress fields are described as 1.2.1 and 1.2.2 with A' instead of A. For all events in the construction sequence we can think of similar incremental displacements and stresses. By some method of adding these incremental solutions the displacements (U_i) and stresses (σ_{ij}) in the final completed body may be evaluated. This summation process must be such that it takes into account the relationships between displacements, stresses and time which characterize the material of the fill. The simplest such material description would be one that is linearly elastic and where this response is independent of time.

For the simple directly elastic material which is independent of time the conditions at the point of interest jump as each incremental layer is added but remains constant between such additions.

When the construction is continuous then the final conditions at C, a point of interest, are represented by

$$U_i = \int_C^F \tilde{U}_i dL \quad 1.2.3$$

$$\sigma_{ij} = \int_C^F \tilde{\sigma}_{ij} dL \quad 1.2.4$$

where F is the final contour and dL an increment of added material.

When the material response depends upon certain existing conditions in the body, such as the existing stress or strain level, but is still independent of time, then this response characteristic will vary from point to point in the already constructed body. The

incremental function for an elemental increase in level at a point will depend not only on the material properties at that point but also on the properties everywhere else in the body. This means that the response at C depends on the cumulative functions everywhere in the body. Clearly with the addition of the dependency upon time the problem is further complicated and solutions for only very simple configurations and highly idealized material laws may be possible.

In the linear elastic case we formally seek \tilde{U}_i and $\tilde{\sigma}_{ij}$ fields which are compatible, in equilibrium and satisfy the boundary conditions. By processes such as 1.2.3 and 1.2.4 the final conditions are arrived at and these results are in equilibrium and satisfy the final boundary conditions but are not necessarily compatible. The possible presence of the incompatibility tensor must be associated with the boundary conditions prescribed for the additional layer in the incremental solution. Acceptable conditions on a horizontal surface would be normal tractions of magnitude given by weight/unit area of the added material and no tangential tractions. This means that slip between the existing body and the added layer is possible but with the addition of a subsequent layer the boundary is shifted up and the original added material becomes an intrinsic part of the body. By this process, a dislocation of the Somigliana type is formed at each new upper boundary; with the subsequent addition of material this dislocation is healed but the conditions for the existence of an incompatibility tensor exist. Certainly, no holes or breaks exist in final body and under certain conditions the Beltrami-Michell conditions could be

satisfied. These conditions would involve no tangential slip at an incremental upper boundary and may not be realistic.

Complete solutions for incremental problems of bodies built-up in a gravity field are available for a sphere and for an embankment with infinite sides. In each case the important physical difference between the incremental results and those where the effects of inertia are applied as an external condition to the completed body have been demonstrated. In certain problems, where no dislocations at the incremental surface exist, these differences will not occur and the final solutions will be compatible. A trivial case of this is the quarter plane, where the increments are applied in parallel, horizontal layers. It should be noted that the normal uniqueness theorems in classical elasticity must be extended to account for the building order in cases where the final gravity body forces occur in an incremental manner.

The object of the incremental analysis of the gravity conditions in embankments was to develop a mathematical model which had the usual abilities to determine stresses and strains but which also could account for the history of construction. In a similar manner this historical element is of importance with respect to the culvert. The variability of the conditions in the completed embankment depends upon the manner and sequence of construction. By much the same argument the tractions on the surface of an enclosed culvert will also depend upon these events. The structural problem is to design a culvert for given loadings whereas the problem undertaken here is to find methods

of prescribing the stress field. In this sense the same approach as described in considering the conditions in embankments is valid.

1.3 Formulation of Incremental Problem for Computer Solution

The problem discussed in the previous section may be physically understood by considering a body partially completed, which is loaded over a part of the surface by a layer of material which exists only within the bounds of the final configuration. The fields $\tilde{U}_i(x_i)$ and $\tilde{\sigma}_{ij}(x_i)$ described the effects of this layer. In linear elasticity the incremental solutions must satisfy the equilibrium and compatibility conditions, the boundary conditions on the completed part of the boundary as defined by the method of supports, and those on A imposed by the material layer. These latter conditions may be

$$\tilde{\sigma}_{yy} = -\rho g \Delta, \quad \tilde{\sigma}_{xy} = 0 \quad (1.3.1)$$

on A, where Δ is the layer thickness and ρg the material density. Physically these conditions refer to constant normal tractions and no shear cohesion along the loaded surface. It is the latter which sets up the conditions for a Semigliana type dislocation and the final incompatibility tensor. The incremental solutions $\tilde{\sigma}_{xx}, \tilde{\sigma}_{xy}, \tilde{\sigma}_{yy}, \tilde{U}_x, \tilde{U}_y$ are required at a point of interest C(x,y). Such solutions may be changed to account for a differential layer where $\sigma_{yy} = -\rho g dY$ in 1.3.1, where Y is the location of the layer A. By integration for all Y from C at Y=y to the final contour F the effects of the gravity conditions and the manner of construction can be modelled. In this case we choose the finite element method for plane elasticity problems as

developed by Clough for an approximate solution. This is fully described in the literature but some restatement of the work is necessary for the application to incremental problems.

As in Fig. 2, the whole body is divided into contiguous triangles which approximate the final configuration and some of the incremental surfaces to which material is added in the actual construction procedure. Such surfaces are A_1, A_2, A_3, A_4, A_5 , at locations Y_1, Y_2, Y_3, Y_4, Y_5 in Fig. 2, and we are interested in the conditions at C, a fixed point. To determine these the effects of a unit load per unit x added along each surface A_1 to A_5 is necessary. This load is equivalent to a density of unity and an increment, Δy , of unity. The effects at C may be plotted for various Y and the final curve gives an influence line for the conditions at C due to a unit load over a horizontal surface, bounded by the body configuration, at Y . The ordinate is the influence density at C. Such a plot is shown in Fig. 3 where the accuracy of the line depends upon the closeness of the loaded surfaces. Clearly for $y \leq Y_1$ the influence density is zero. In order to determine the final conditions at C we must multiply each ordinate by the local material density at each Y and find the area under the resulting plot from $y = Y_1$ to $y = Y_F$. If the material density is constant then the final condition for vertical displacement has the form

$$U_y = \rho \int_{Y_1}^{Y_F} f(y) dy \quad 1.3.2$$

where f is influence density for this displacement. The integration 1.3.2 can be carried out numerically -- an operation the computer is well suited to. Similar expressions to 1.3.2 exist for the stresses and horizontal displacements.

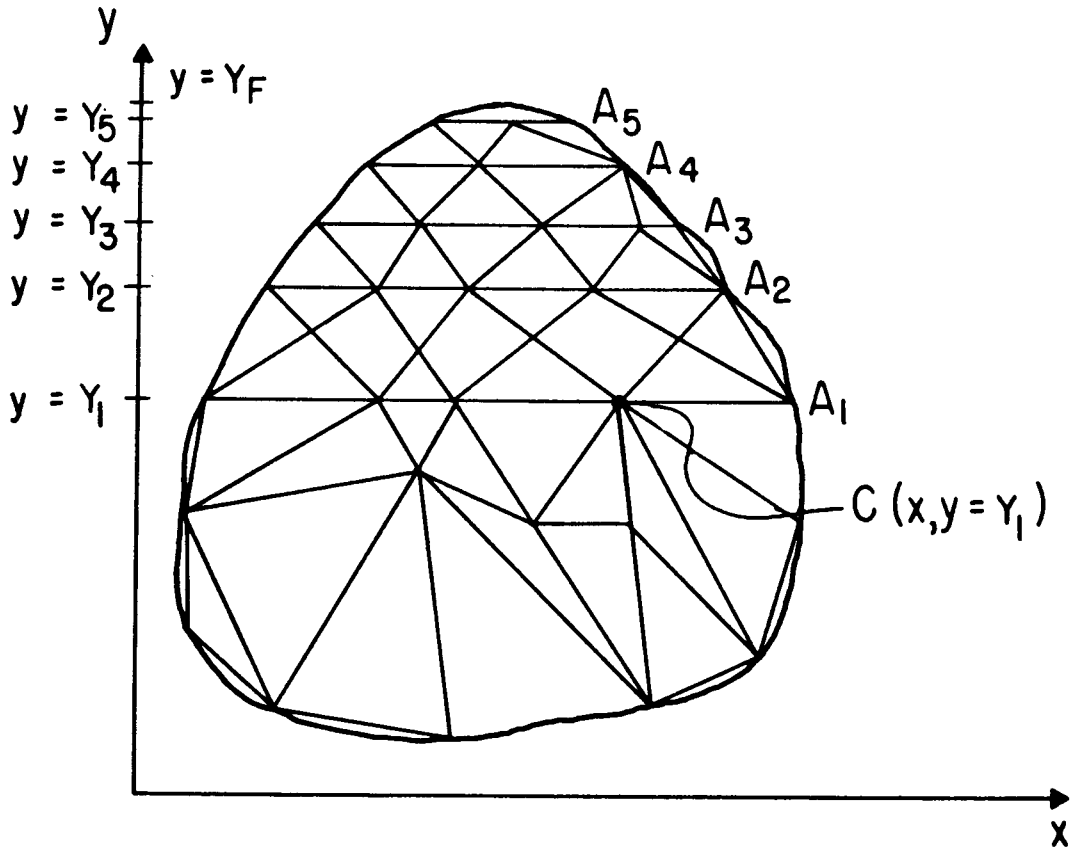


FIG. 2

TYPICAL ELEMENT ARRANGEMENT

INFLUENCE
DENSITY
FOR
STRESS
OR DIS-
PLACEMENT
AT C

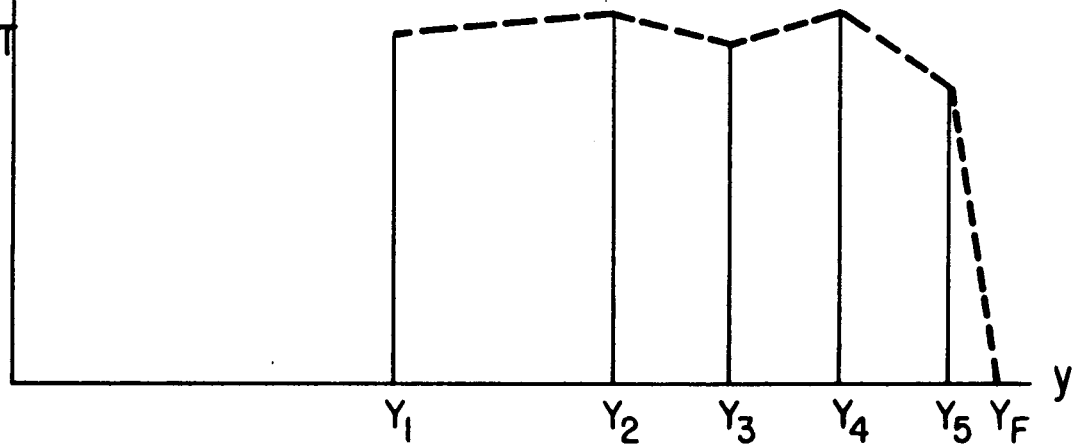


FIG. 3

TYPICAL INFLUENCE DENSITY CURVE

1.4 Other Considerations in the Analysis

Although the embankment with included culvert is a three dimensional system it was found convenient to consider a unit thickness slice plane with normal along the culvert longitudinal axis (the z-axis in Fig. 1) in the region of the center of this axis length. This slice only sustained in-plane displacements and the resulting theoretical simplification allowed relevant results to be obtained. Justification must be sought for this slice assumption. The cross section considered would, in many embankments, have nearly symmetric geometrical conditions about a vertical axis (the y-axis in Fig. 1) through the culvert. The section in the center of the z-axis also may possess symmetry about the plane of the slice. The predominance of the soil weight effect would result in zero displacements in the direction of the z-axis if these symmetries exist and any deviations from these symmetries tend to vitiate the in-plane assumptions.

The material properties are assumed to be linearly elastic in all of this work. The problem is not linear because of the incremental dislocations occurring at each soil layer. In addition, Brown and King⁵ have shown how non-linear stress:strain law materials may be dealt with provided that they satisfy certain restrictions which are termed of the Markov type. The restriction involves considering only the linear elastic effect of a small change in either force or displacement field where the slope of the stress:strain curve depends upon the existing state of strain at incipience of the change. This

state of strain varies over the whole body and therefore the local modulus is spatially dependent but quite independent of history and time.

An additional problem exists because the embankment fill is superimposed onto the earth's surface, which deforms because of this overload. These deformations may considerably affect the conditions in the fill and around the culvert. The case of a load on a semi-infinite body has been most thoroughly investigated and the relative physical meanings of various mathematical models has been investigated by Kerr.⁶ In this work three approaches were made to the problem and the results compared.

- 1) Treating the earth's surface as rigid (Fig. 4a).

- 2) Selecting a rectangular linearly elastic, massless block of the earth, containing the embankment and with boundary conditions on the block of zero horizontal displacements on the base and sides, zero vertical displacements on the base and zero shear tractions on the sides (Fig. 4b).

- 3) As (2) except the boundary conditions on the base are for continuity of normal and shear stresses and the base is a part of a semi-infinite body of the same properties as the block (Fig. 4c).

The choice of the boundary and interface conditions was based on reasonable physical expectations. In addition, the fixed and fixed in the normal and free in the tangential displacement conditions were well suited to the finite element approach. The conditions of (3) were treated by a method due to King⁷ by which influence coefficients on the horizontal boundary were generated for horizontal and vertical

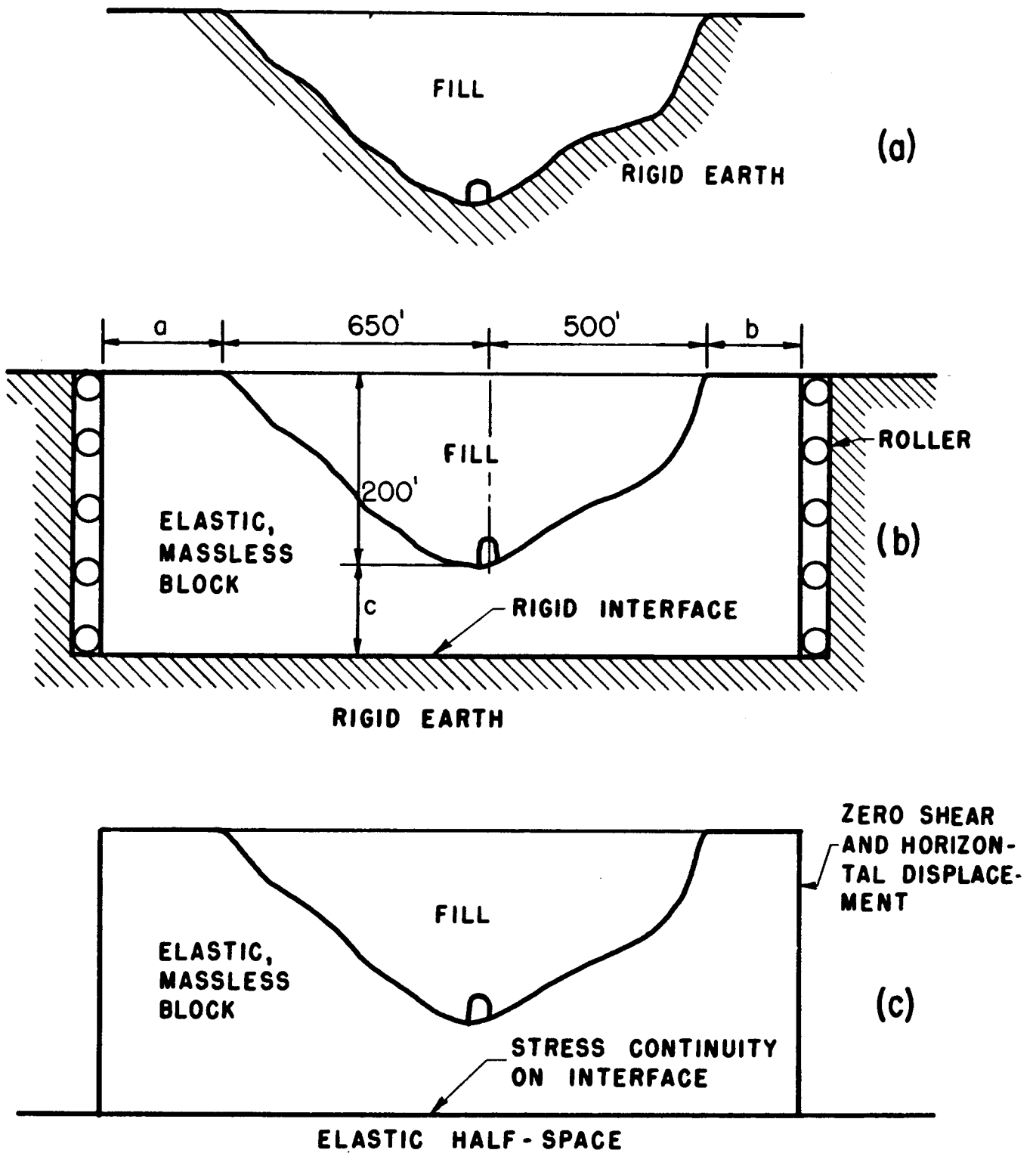


FIG. 4

ROCK BOUNDARY CONDITIONS

loads on the boundary. These influence coefficients were based on Boussinesq and Carrutti type equations for the plane.

In general, the culvert was considered to be rigid, but in order to obtain an impression of the effect of the displacements of the culvert the volume enclosed by the outside culvert boundary could be considered to have a definite stiffness. The change in tractions determined for flexible culvert could be compared to the rigid case. Much of the previous discussion was concerned with the history of placing the soil in the embankment. Another important practical facet of the problem concerns the effect of placing an area of very weak material over the crown of the culvert. Intuitively this tends to cause the thrust to "arch" over the weak material and reduce the force on the top of the culvert. The presence of the weak material is realized in the field by filling to about 12' above the culvert top, removing this material above the crown and replacing with straw or other organic material. This history of events is idealized in the mathematical model by carrying out the incremental technique to the required level above the culvert crown, determining the tractions (normal and shear) around the edge of the proposed excavated region, solving the boundary value problem where these tractions, reversed in sign, are applied to the previously obtained incremental solution. This results in the stage of construction where the excavation of the region over the crown is completed. The added organic material is considered to cause pressures on the base of the excavation equal to its own head. On the sides contact between the normal fill material and the organic material is

considered to exist; with subsequent addition of fill above the boundaries of the normal fill to the organic material as continuity of strains and the relatively low stiffness of the latter induces the so-called "arching" action.

Final sets of interface conditions between the fill and the culvert, and the fill and the earth's surface require decisions. The culvert was assumed to be a finite element mesh with very high stiffness to simulate the rigid inclusion. As previously mentioned this stiffness could be reduced in order to determine the gross effects of culvert flexibility on the load distribution on the barrel. The outside boundary of the culvert (barrel) was assumed to transmit only normal tractions and this condition was provided by linking the nodal points of the finite elements on the barrel to the fill nodal points by triangular elements one nodal point of which was free and the opposite side joined the culvert to fill by a line normal to the barrel. The fill-earth interface was considered to be rough with the maintenance of contact points. Naturally, it is difficult to defend these interface conditions, but, without more extensive experimental evidence than presently exists, some extreme assumptions must be made.

The original geometry was assumed to be unaltered for all incremental solutions. This is a reasonable statement for the inclusion and the earth's surface. However, the compression of the fill under its own weight as the construction process continues exists but is not predictable from normal elastic analysis.

1.5 The Effective Modulus of the Fill

The fill for the San Luis relocation was obtained from borrow pits and highway excavation close to the site and consisted of rocks varying from 2" to over a foot diameter distributed in a sand-clay matrix. This conglomerate was typical of that often found in such earth structures and methods of determining the modulus of elasticity employed in design is of some general interest. Clearly the testing by static means of a typical specimen is impossible; the dimensions of such a specimen ensure that the cutting, design and operation of test would be beyond present facilities normally available. The necessity of obtaining a sufficient number of specimens to ensure a reliable statistic of the gross or effective modulus further aggravates the problem. Various theoretical methods are available to estimate the effective modulus of such a conglomerate. These involve knowledge of the aggregate modulus, matrix modulus and the amount of aggregate of each type by size and material property in a given volume. The bounds on the effective shear and bulk modulus obtained by Hashin³ are applicable to this problem and the less restrictive, simpler bounds by Hashin and Shtrickman⁴ for more general materials are also relevant. This bounding is made possible by clever variational theorems and it is these works which will be utilized here. The theorems have been applied to alloys of carbide particles embedded in a cobalt matrix where results show theoretical bounds which are close together and experimental values for the effective modulus, E , which fall within these bounds.

In the determination of the effective properties of the fill it was found possible to determine statistics on the shear and Young's modulus of the soil and rock inclusions, together with an indication of the amount of rock between various equivalent spherical dimensions within a unit volume of the conglomerate. This information was applied to the equations of references 3 and 4 for the evaluation of effective moduli.

We will consider the material idealized to spheres of varying diameters and elastic properties enclosed in uniform elastic matrix. The spheres are considered to be spread through the medium in a random manner so that there is no tendency to bunch together and every sphere is surrounded by the matrix. The conditions for this arrangement and a rule for the distribution of spheres as the terms in a Poisson process is discussed elsewhere.⁵ It is necessary to assign to each sphere an associated volume of matrix and for this purpose the arrangement where

$$c = \frac{1}{V} \sum_{i=1}^n \sum V_i^s = \frac{V_i^s}{V_i} = \sum_{i=1}^n c_i \quad 1.5.1$$

and $c_i = \frac{1}{V} \sum V_i^s$, may be descriptive. Here we think of n types of stones (where each type is associated with common elastic properties and diameter) of individual volume V_i^s and add all the stones of each type and all the types together, which sum, when divided by the total body volume V, gives the parameter c. In the small we may think of the stone V_i^s being surrounded by matrix such that the volume of stone and associated

matrix, V_i , divided into V_i^S also gives the descriptive parameter c .
 If the total volume V is too large for these measurements to be carried out then samples may be used to determine a statistic for c .

Considering the work of Hashin and Shtrickman for a general material, that is one with no predominant matrix material, then

$$K_u = K_n + \frac{A_n}{1 + \alpha_n \frac{A_n}{A_n}} \quad 1.5.2$$

$$K_L = K_o + \frac{A_o}{1 + \alpha_o \frac{A_o}{A_o}} \quad 1.5.3$$

where $K_u \geq K^* \geq K_L$

and

$$G_u = G_n + \frac{1}{2} \frac{B_n}{1 + \beta_n \frac{B_n}{B_n}} \quad 1.5.4$$

$$G_L = G_o + \frac{1}{2} \frac{B_o}{1 + \beta_o \frac{B_o}{B_o}} \quad 1.5.5$$

where $G_u > G^* > G_L$

Here K^* and G^* are actual effective bulk and shear moduli of the polyphase material, K_u and G_u are upper bounds and K_L and G_L lower bounds. As no definite matrix need exist in this material K_o and G_o are defined as the smallest moduli and K_n and G_n the largest.

Therefore, $\sum_{i=0}^n C_i = 1$ and in addition

$$A_j = \sum_{i=0}^{j-1} \frac{C_i}{\frac{1}{K_i - K_j} - \alpha_j} + \sum_{i=j+1}^n \frac{C_i}{\frac{1}{K_i - K_j} - \alpha_j} \quad 1.5.6$$

$$B_j = \sum_{i=0}^{i=j-1} \frac{C_i}{\frac{1}{2(G_i - G_j)} - \beta_j} + \sum_{i=j+1}^{i=n} \frac{C_i}{\frac{1}{2(G_i - G_j)} - \beta_j} \quad 1.5.7$$

$$\alpha_j = - \frac{3}{3K_j + 4G_j} \quad 1.5.8$$

$$\beta_j = \frac{\alpha_j}{5G_j} (K_j + 2G_j). \quad 1.5.9$$

Clearly, if we consider C_o , K_o , G_o as referring to the matrix and properties from 1 to n as the inclusions (where the matrix, as is usual in practice, has the lowest properties) then we arrive at bounds for the case described by 1.5.1.

For the special structure material of 1.5.1, where both matrix and inclusions are defined, these bounds may be closed to

$$K_u = K_o + (3K_o + 4G_o) \sum_{i=1}^n \frac{(K_i - K_o)C_i}{4G_o + 3 \left[K_i - (K_i - K_o)C_i \right]} \quad 1.5.10$$

$$K_L = K_o + (3K_o + 4G_o) \sum_{i=1}^n \frac{(K_o - K_i)C_i}{3K_i + 4G_o \left(1 - C_i + \frac{K_i}{K_o} C_i \right)} \quad 1.5.11$$

$$G_u = G_o \left[1 + \sum_{i=1}^n \left(\frac{G_i}{G_o} - 1 \right) C_i \theta_i \right] \quad 1.5.12$$

$$G_L = G_o \left[1 - \sum_{i=1}^n \left(\frac{G_i}{G_o} - 1 \right) C_i \phi_i \right]^{-1} \quad 1.5.13$$

where θ and ϕ are defined in Appendix A. For $i=1$, $K_u = K_L = K^*$ in 1.5.10 and 1.5.11. It is to be noted that this is an exact value of

the effective bulk modulus only for the idealized spherical inclusions where the strain energy in all the spheres of volume V_i approach the strain energy in conglomerate. Hill⁹ terms this as an arrangement of "spherical composite elements". Also, when $i = 1$, $K_u = K_l = K^*$ in 1.5.3 and 1.5.4 under the circumstance that $G_0 = G_1$, that is when only the bulk moduli differ.

With bounds on the bulk and shear effective moduli determined, it is possible to find the effective Young's modulus from

$$E = \frac{9KG}{3K + G} \quad 1.5.14$$

The additional complications for the closer bounds in 1.5.10-13 do not allow a convenient statement when the material is described as in 1.5.2. However, in the description of 1.5.2-5 a simple statement is possible. Two types of material specification will be considered, first where the curve of Fig. 5 describes the entire content, i.e., when c in 1.5.2 is unity, and second when the material of the curve is enclosed in homogeneous matrix, $c < 1$. For both specification types it is possible that the material elastic properties are not constant. Some variation as in Fig. 5 may exist and it is necessary to describe this as a function of V^s . For instance for Fig. 5 we may state

$$K(V^s) = \frac{K_1}{2} \left\langle V^s - V_1^s \right\rangle^0 + \frac{K_1^2}{2} \left\langle V^s - (V_1^s + V_2^s) \frac{1}{2} \right\rangle^0 \quad 1.5.15$$

Under the circumstances we may form functions

$$a_j(V^s) = \frac{f(V^s)}{\frac{1}{K(V^s) - K_j} - \alpha_j} \quad \text{and} \quad G_j(V^s) = \frac{f(V^s)}{\frac{1}{2(G(V^s) - G_j)} - \beta_j}$$

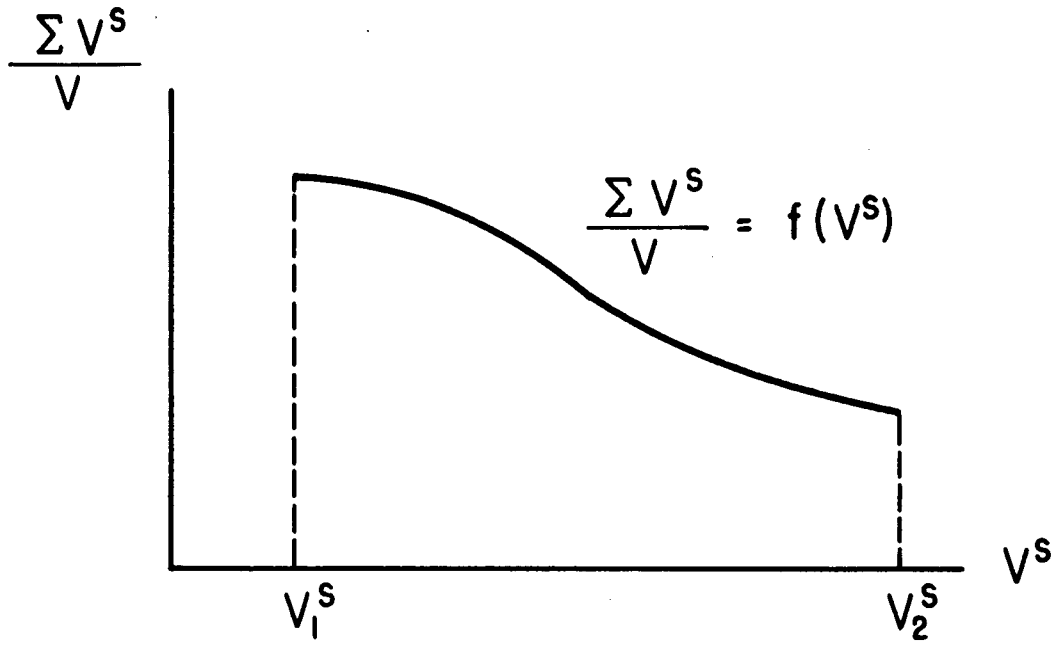


FIG. 5

INCLUSION GRADING CURVE

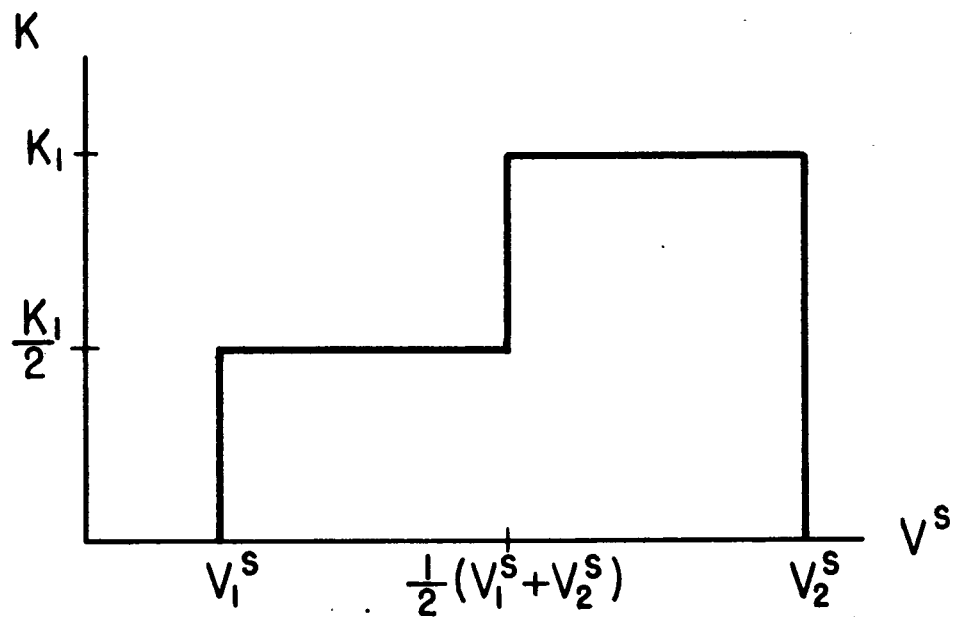


FIG. 6

STEP VARIATION OF MODULUS WITH V^S

which allow us to describe

$$A_n = \int a_n(V^S) dV^S \quad \text{and} \quad B_n = \int b_n(V^S) dV^S \quad 1.5.16$$

where the integrations are over all material with moduli smaller than K_n and G_n respectively as in 1.5.2 and 4. Also for integrations for all material in excess of K_0 and G_0 in 1.5.3 and 5 we may describe A_0 and B_0 as in 1.5.16 with exchanged subscripts.

In the second type of specification, where the matrix occupies a volume V_0 with elastic properties K_0 and G_0 , 1.5.16 becomes

$$A_n = \frac{\frac{V_0}{V}}{\frac{1}{K_0 - K_n} - \alpha_n} + A_n(V^S) dV^S \quad \text{and} \quad B_n = \frac{\frac{V_0}{V}}{\frac{1}{2(G_0 - G_n)} - \beta_n} + b_n(V^S) dV^S \quad 1.5.17$$

where the integrations are over the volume of inclusions with moduli smaller than K_n and G_n respectively. For use in 1.5.3 and 5,

$$A_0 = \int_{V_1^S}^{V_2^S} a_0(V^S) dV^S \quad \text{and} \quad B_0 = \int_{V_1^S}^{V_2^S} b_0(V^S) dV^S \quad 1.5.18$$

1.6 Synthesis

This part of the report has drawn together various theoretical and formulations necessary to attach analytically the conditions on a built up embankment with a culvert inclusion. It is necessary now to organise the treatment having in mind the previous discussions.

The incremental analyses for gravity stresses treated in other works is adapted for the finite element approximate solutions in plane elasticity. Instead of thinking of the superposition of material as a continuous process, the effects of additional material in discrete

layers is determined and the conditions associated with the final configuration are found by an approximate summation process. The effects of a layer of material require that the foundation reaction, the material properties of soil-rock matrix and the response due to organic material be studied. To deal with the foundation reaction various methods are proposed. Each involves some idealization of the actual conditions, the extent of which can be completely discerned. The elastic properties of the rock are determined from cores. Those of the soil-rock conglomerate are closely bounded by methods due to Hashin. These bounds require knowledge of the elastic properties of the soil, inclusions and the percentage of volume of inclusions compared to the total volume for various rock sizes. This information must be obtained empirically.

PART II

SAN LUIS RESERVIOR ROAD RELOCATION EMBANKMENT

2.1 General Considerations

Theory outlined in the previous part is now applied to the particular embankment, with enclosed culvert, on the San Luis Reservoir road relocation. The first point of interest is the distribution of forces around the barrel and second the tractions in the fill. The barrel forces are of importance to the structural designer of the culvert and knowledge of the predicability of soil stresses is always of concern. Extensive instrumentation was carried out to check these analytical results. In this part of the report the actual bounds on the fill properties are described, the computer analysis specified and a description of the problems of instrumentation given.

2.2 Material Properties

The assumption of a rigid culvert ensured that the material properties of this element were defined. However, as an additional matter an investigation of the general effects of culvert deformations was made and for this purpose the body enclosed by the barrel was given a definite material stiffness of

$$E \text{ culvert} = 2.9 \times 10^6 \text{ p.s.i.}$$

$$\nu \text{ culvert} = 0.4.$$

The properties of the existing rock (a sandstone) on which the fill was placed were obtained from bore hole specimens at various depths. Two

types of tests were conducted:

- a) Static compression on specimens about 3" long and 2" diameter.
- b) Dynamic bending and longitudinal oscillations on specimens about 13" long and 2" diameter.

In the static tests, eleven specimens were finally used. Other specimens shattered in early test because of faulting, or broke in the end capping process. The static modulus of elasticity varied from 6.6×10^6 p.s.i. to 3.9×10^6 p.s.i. The mean was 4.8×10^6 p.s.i. and the standard deviation 15%. In the same tests lateral strains were measured and the value of Poisson's ratio varied between 0.11 and 0.14. The stress-strain curves were essentially linear up to 7,000 p.s.i. and then strain softening. The stress: Poisson's ratio curves indicated a constant value of the ratio up to 7,000 p.s.i. and then increasing values to 0.18 at 10,000 p.s.i.

The dynamic measurements were associated with the determination of the flexural and longitudinal wave frequencies. The former was much more dominant and easily determined. Two specimens were tested in each mode. The dynamic modulus of elasticity figures were 6.25 and 4.75×10^6 p.s.i. in bending, and 7.3 and 5.8×10^6 p.s.i. in the longitudinal motion.

The stresses in the base rock were not expected to exceed the linear static response and the values from these tests were employed in the analysis. The difficulty in deciding the flexural critical frequencies and the confirmation of the static results by the bending wave dynamic tests encouraged the use of the mean static modulus. The results for Poisson's ratio from static tests also were consid-

ered satisfactory and in the analysis the following rock elastic properties were employed:

$$E \text{ rock} = 4.8 \times 10^6 \text{ p.s.i.}$$

$$\nu \text{ rock} = 0.12$$

The embankment fill material was composed of adjacent excavated material and consisted of the rock previously described and soil which formed the matrix in which the rock was carried. The conglomerate had water added to the extent of the optimum water content of the soil. Bounds on the modulus of elasticity were obtained by the methods of section 2.5. Two additional pieces of information beyond that already described were required:

- a) The soil elastic properties.
- b) The arrangement of the rock inclusions.

The determination of the elastic modulus of the soil was obtained from two test results on each of three samples taken from widely different parts of the fill. The stress strain curves were obtained on specimens re-moulded at the optimum water content. The first quarter cycle of the loading was employed in the modulus determination and this was justified by the realization that the loading produced an essentially monotonic increase in strain with addition of fill material. The load deformation curves from the unconfined compression test were essentially linear up to a stress of 60 p.s.i. The tests were of the strain type at a rate of 0.02 in./min. The independent tests of the same samples provided confirmation of the sample modulus but the different samples

had widely varying results, namely values 7.7, 4.3 and 16.0 k.s.i. The average

$$E_{\text{matrix}} = 9.3 \times 10^3 \text{ p.s.i.}$$

The value of Poisson's ratio was difficult to determine from tests. However, a technique using the methods of Paul¹⁰ where

$$E^* = E_c + (E_p - E_c) A_p \quad 2.2.1$$

$$G^* = G_c + (G_p - G_c) A_p \quad 2.2.2$$

hence

$$G^* = G_c + (G_p - G_c) \frac{(E^* - E_c)}{E_p - E_c} \quad 2.2.3$$

provides practical results. Now the soil consists of clay and pieces of small sandstone the properties of which have been described. When the rock particles were washed out the value of the clay modulus was found to average 7.1 k.s.i. = E_c . Assuming $G_c = \frac{E_c}{3}$ and knowing $E^* = E_{\text{matrix}}$, $G_p = \frac{E_{\text{rock}}}{2(1 + \nu_{\text{rock}})} = 2143 \text{ k.s.i.}$, then

$$G^* = \frac{7.1}{3} + (2143 - \frac{7.1}{3}) \frac{(9.3 - 7.1)}{4800 - 7.1} = 3.3 \text{ k.s.i.}$$

but
$$\nu^* = \frac{E^*}{2G^*} - 1 \quad 2.2.4$$

hence
$$\nu^* = \nu_{\text{matrix}} = 0.4 \ddagger$$

With these results for the rock and soil modulus and Poisson's ratio

[‡]This argument was devised by N. Mostaghel.

the bounds for a single inclusion type were found using 1.5.10 through 1.5.13 for various c . These bounds are shown on Fig. 7.

The bounds shown on Fig. 7 indicate only one size of rock inclusion. In fact, an elaborate rock count carried out by the State showed a range of rock sizes. Even this rock count was made before the compaction of the material in the fill was carried out and definite reduction in sizes would have occurred in this process. Rather than give an impression of spurious accuracy, average values based on one rock size were computed for the inclusion concentration. Two counts were made by the state at widely differing levels in the fill. Material passing a 2" sieve was considered to be a part of the matrix and larger rocks as inclusions. Each count consisted of five loads of about 25 cubic yards each. The loads of each count were obtained from different locations at the same level. Average results are given in Table 1. The mean size of inclusion was a sphere of 5" diameter and the volume concentration was

Count	Average Number of Rocks per Cubic Yard		
	Retained on 2"	Retained on 12"	Larger than 24"
1	477	1	1/2
2	445	1	1/2

Table 1 - Rock Count Results

0.7. With this value of C the bounds on the modulus are determined from Fig. 7. The mean was used for the modulus and Poisson's ratio of the matrix was considered to govern.

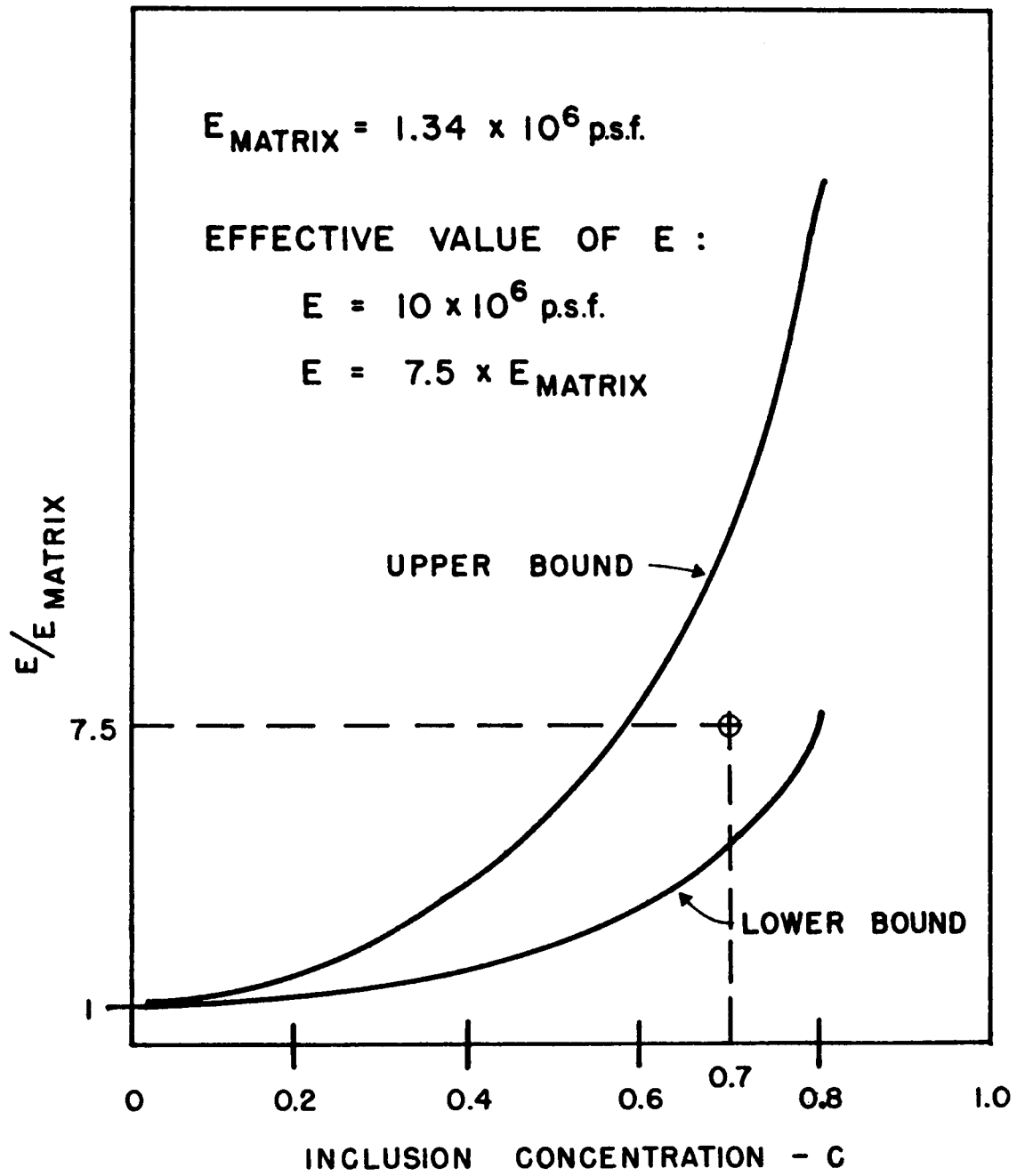


FIG. 7

BOUNDS ON E

This lower bond has been shown to be a dubious value¹¹. Under these circumstances lower values may be more pertinent and a range employed in the analysis is shown on Fig. 8.

2.3 Computer Analysis

The example refers to the system indicated in Fig. 1. It is the arrangement in a road relocation required by the creation of the San Luis Reservoir near Los Banos, California. The values of material properties employed in the analysis are shown in Fig. 8.

In order to account for the incremental character of the material placing nine steps were considered in the analysis. A schematic of these is shown in Figure 8. For each the effects of a uniform load at that surface were found and used as influence densities for the final integration process. This process utilized a simple trapezoidal rule. The effects of the inclusion of the organic material were accounted for in the manner previously described between layers 3 and 5. The stress and displacement fields were determined on the assumption that the organic material was continuous with the main fill on its boundary, but that its weight was transferred only by normal forces at its base.

The effects of the various rock boundary conditions shown in Figure 4 were considered as follows:

- a) The arrangement of Figure 4(b) was compared to those of Figure 4(c) with a coarse finite element mesh. The stresses in the vicinity of the culvert inclusion were nearly identical by both schemes of investigation. The arrangement of Figure 4(c) was therefore not used because of the increased computer demands of such a system.
- b) The determination of a, b and c in Figure 4(b). The realization of the minimum value of these dimensions is important because it

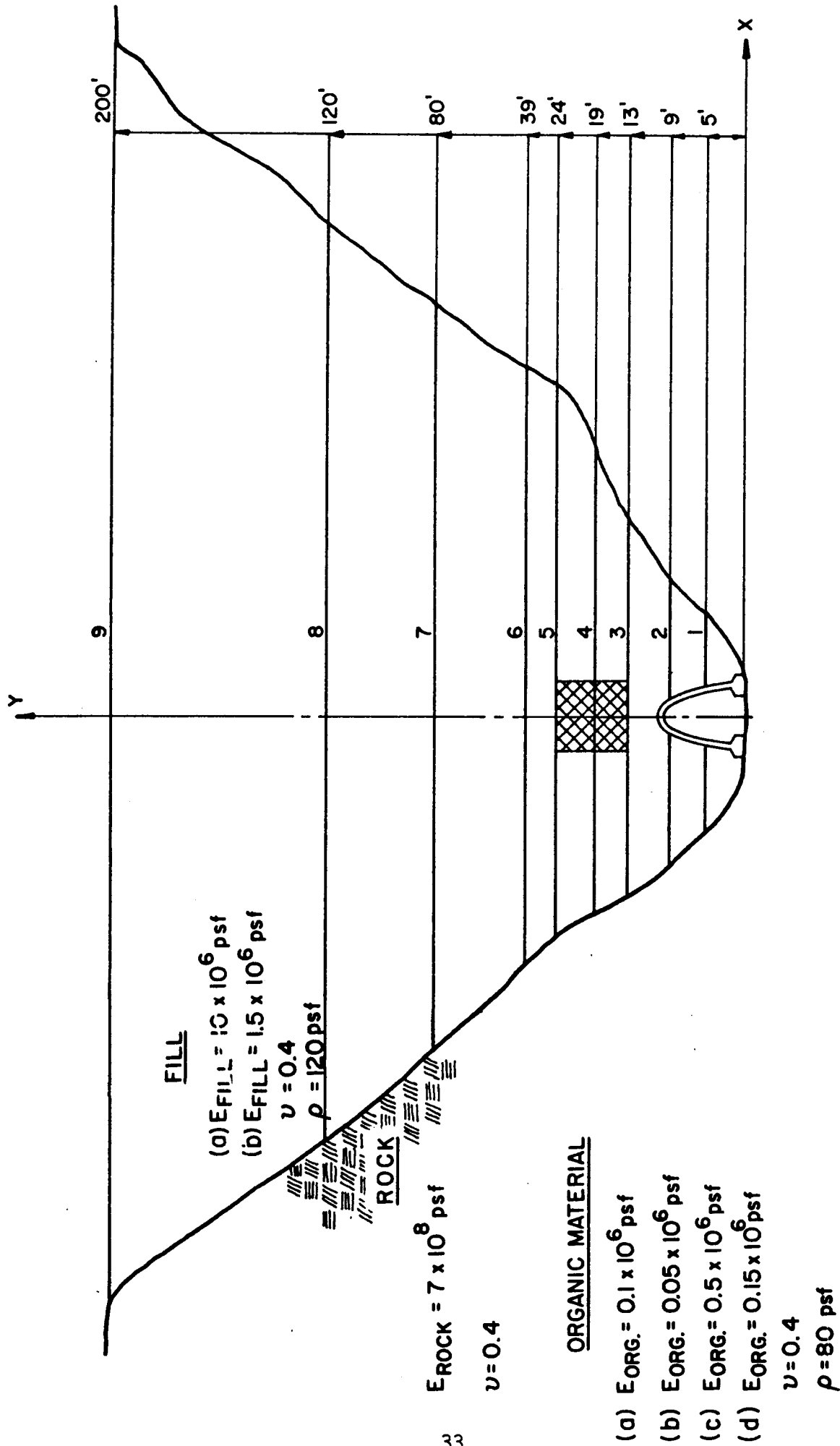


FIG. 8

SCHEMATIC OF EMBANKMENT

allows a finer mesh to be used with subsequent increased local accuracy.

Many block sizes were compared and the figures

$$a = 650'$$

$$b = 600'$$

$$c = 200'$$

were finally selected. For a larger block little change in the fill stresses was observed. Seven full analyses were run as shown in Table II.

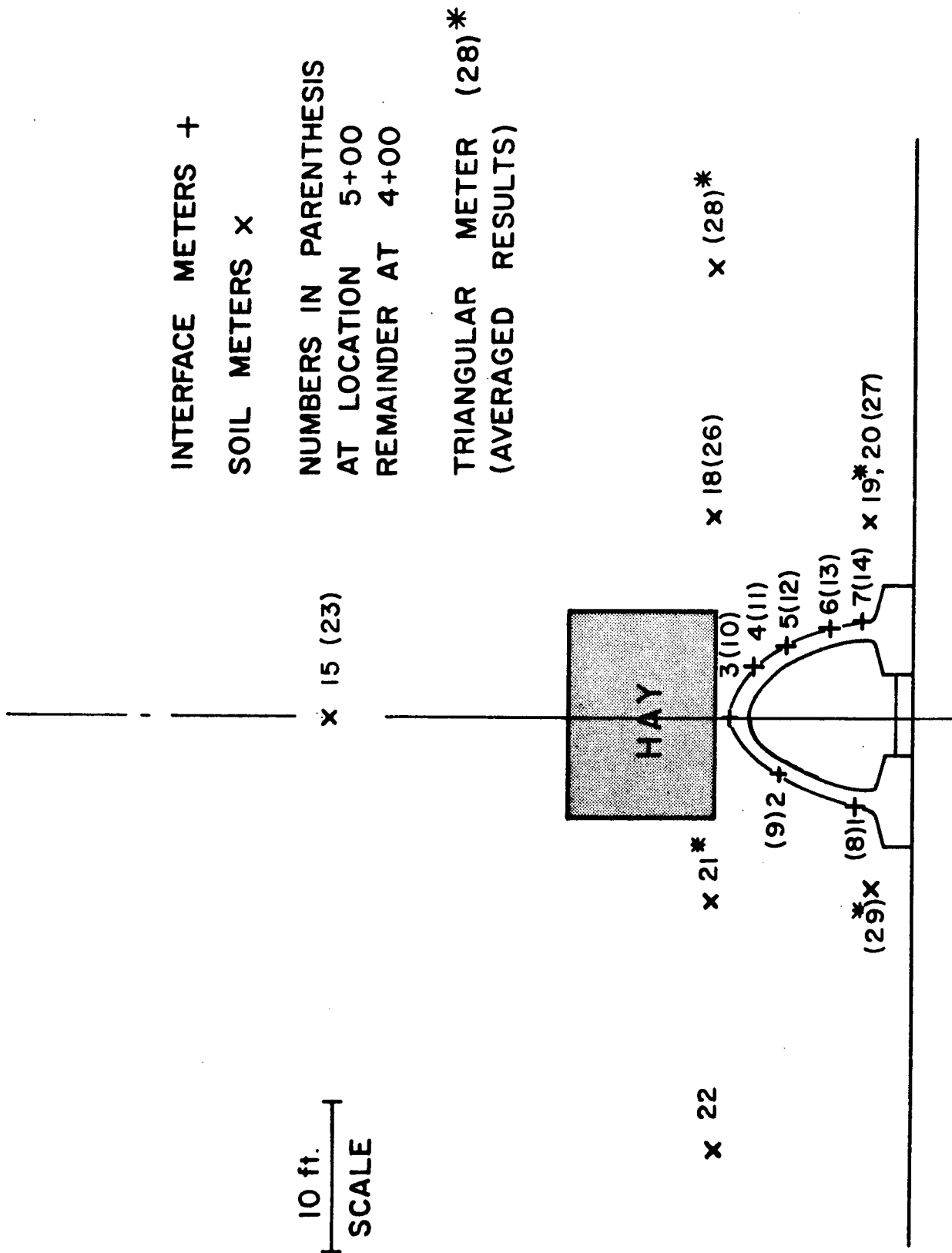
Analysis Number	Rock Boundary (Fig. 4)	Fill (Fig. 8)	Hay (Fig. 8)	Ratio: $\frac{\text{Fill}}{\text{Hay}}$ modulus
1	Rigid (a)	(a)	No hay	1
2	Rigid (a)	(a)	(a)	100
3	Rigid (a)	(a)	(b)	200
4	Flexible (b)	(a)	No hay	1
5	Flexible (b)	(a)	(a)	100
6	Rigid (a)	(a)	(c)	20
7	Rigid (a)	(b)	(d)	10

Table II - Analyses Reported

The organization of computer work is indicated in the flow chart and program contained in Appendix B.

2.4 Instrumentation

Carlson type pressure meters were provided around the barrel of the arch (7" diameter) and in the fill. Positions and a reference numbering system are given in Fig. 9. Those meters in the fill were of two types:



a) 18" diameter Carlson meters

b) three 7" diameter meters between two 3/4" plates

which provided the same surface area as type (a). The areas of these meters was influenced by the heterogeneous nature of the fill previously described. A decision on the meter area was obtained by the following analytical approach.

Consider the fill material described on page 19 with total volume V made up of n different types of rock inclusions, the total volume of the ith rock type being A_i, and the matrix of volume B. Therefore, from page 19,

$$A_i = \sum V_i^s \quad 2.6.1$$

$$c = \frac{\sum_{i=1}^n A_i}{V} \quad 2.4.2$$

$$A_1 \cup A_2 \cup A_3 \dots \cup A_n = \phi \quad 2.4.3$$

$$\text{and } A_1' \cap A_2' \cap A_3' \dots \cap A_n' = B \quad 2.4.4$$

where the prime denotes the complement and ϕ the empty set. The volume V need not be the total fill but be a sample so large that no doubt as to its mean or average characteristics exists.

A flat area h in the heterogeneous mass is subjected to a normal force P where

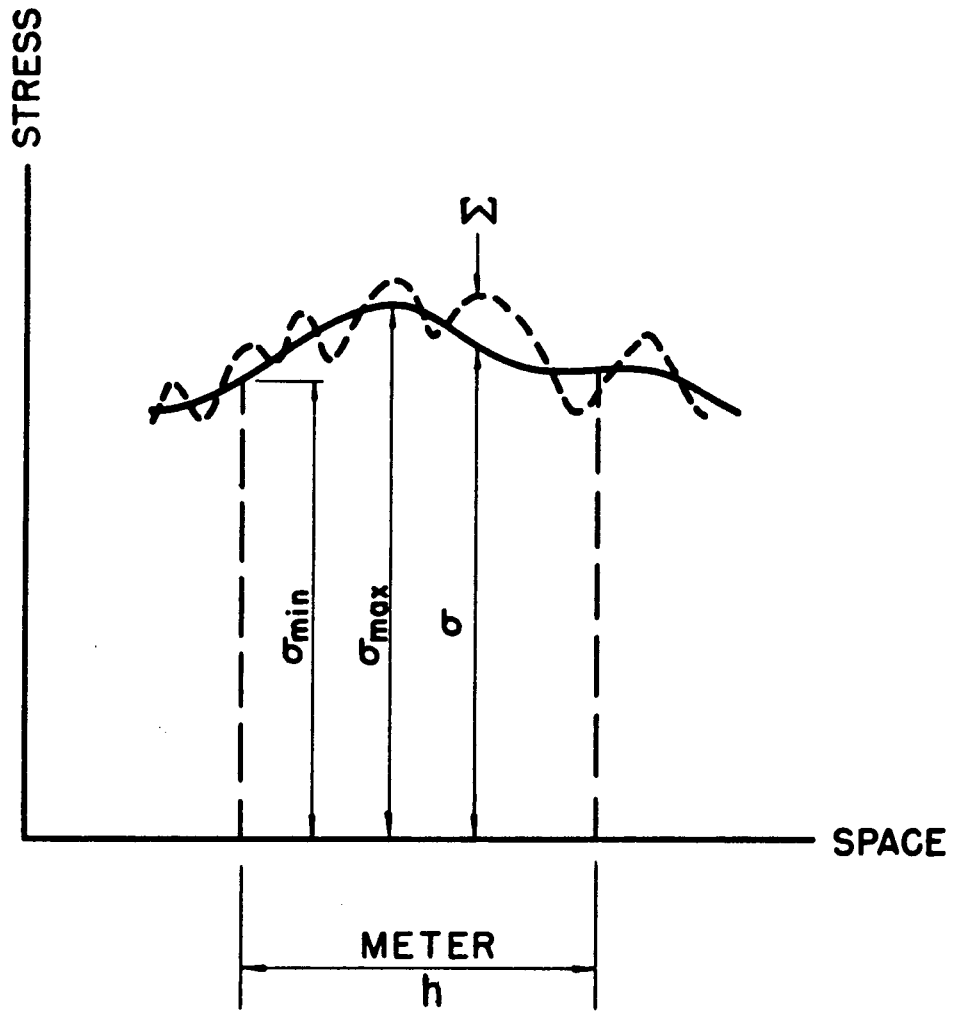
$$P = \int_h \sigma_{nn} \, dh \quad 2.4.5$$

and the average pressure, $\bar{\sigma}_{nn}$, on the area h is

$$\bar{\sigma}_{nn} = \frac{1}{h} \int_h \sigma_{nn} \, dh \quad 2.4.6$$

The local pressure, σ_{nn} , varies across the plane h because of

- 1) The local value caused by the heterogeneous nature of the material.
- 2) The local value associated with the variation of the continuum stress field across such a finite region. Thus Fig. 10 indicates



STRESS VARIATION ACROSS METER

FIG. 10

a variation of the continuum stress field as a continuous curve with the effects of local heterogeneous material riding on it and

$$\sigma_{nn} = \sigma + \Sigma . \quad 2.4.7$$

The problem to be faced concerns the selection of an area h large enough such that the variation due to cause (1) is minimal and small enough that the variation due to cause (2) is also minimal. Again in Fig. 10 the value h sought is such that the change in the extreme continuum values σ_{max} and σ_{min} are small and the effects of the riding values gives

$$\int_h \Sigma \, dh \rightarrow 0 . \quad 2.6.8$$

With this in mind,

$$\bar{\sigma}_{nn} \rightarrow \frac{1}{h} \int_h \sigma \, dh \quad 2.4.9$$

and in addition

$$\frac{\bar{\sigma}_{nn}}{\sigma} \rightarrow 1 . \quad 2.4.10$$

The conditions 2.4.8, 9, and 10 will only approach equalities when σ is uniform and h infinitely large. Here we are interested in quantitative statements on these conditions which will allow us to put confidence in the meter size selected. In addition, the area h must not be considered as just a plane in the material but as an inclusion of a foreign material, the meter, and its effect on the continuum stress field of cause (2) must be included.

Minimum Size

In this part interest is focussed on making the integral in 2.4.8 a minimum. This amounts to taking a sample from V and determining that the sample response is much the same as that of whole body V under the same characteristics as V . This type of problem was investigated by Kelvin¹⁴ who showed that a regular, homogeneous space (in which regular inclusions

occur in a definite array) could be divided up by cells shaped as tetrakaid-ekahedrons, and that these cells would be unrecognizable from each other. In the problem of this communication no such regularity of inclusion array occurs, but, because of their random characteristics it would appear that the basic cell must have point symmetry and, in fact, the sphere would be logical extension to Kelvin's fourteen sided figure. An extreme form of solution would require that the sample set has

$$A_i^S \in V^S$$

where A_i^S are the volume subsets of the rock types in V^S , such that

$$\frac{A_i^S}{A_i} = \frac{V^S}{V} . \quad 2.4.11$$

This means that the inclusions in the sample are in proportional form to the inclusions in the body. Brown⁸ has shown that this is a conservative measure and that the volumes associated with this configuration proportionality are over twenty times larger than required for a stiffness measure of homogeneity. With this in mind, the argument about the minimum diameter of a sample to ensure a measure of stiffness homogeneity follows that of reference (8).

The expected volume of the rock type A_i^S in the sample is

$$E(A_i^S) = A_i \frac{V^S}{V} , \quad 2.4.12$$

but in any sample differing volumes of the rock type will occur in a manner distributed about this value E . A measure of the dispersion of this distribution is the standard deviation, $\sigma(A_i^S)$, which may be normalized into Pearson's coefficient of variation

$$\rho(A_i^S) = \frac{\sigma(A_i^S)}{E(A_i^S)} .$$

An acceptable measure of $\rho (A_i^S)$ is a value k and

$$k = \rho (A_i^S) . \quad 2.4.14$$

Similar equalities may be written for all A_i^S and a region may be described in n -dimensional space by the various

$$(1-k) E (A_i^S) < A_i^S < (1+k) E (A_i^S) \quad 2.4.15$$

in which the probability of A_i^S being in this region is

$$p \left[(1-k) E (A_i^S) < A_i^S < (1+k) E (A_i^S) \right] = P_i . \quad 2.4.16$$

The n probability products of the assumedly independent event A_i^S

$$P_1 \cdot P_2 \cdot \dots \cdot P_n = q . \quad 2.4.17$$

The configurational sample of diameter D_s of volume V^S is one where the n products of 2.4.17 equal an acceptable value q . This is found by the adjustment of the value k in 2.4.14 such that the region in the sphere space of 2.4.15 is specified. This sample is one in which each rock type occurs in much the same arrangement (as indicated by k) as in the body V and in this sense 2.4.11 is satisfied. This is a restrictive statement on D_s and in fact, smaller proportions may be specified by thinking in terms of the stiffness of the sample. An expected effective modulus F^* of the conglomerate may be considered as a function of the moduli of A_i^S and B , and the expected quantities $E (A_i^S)$. Thus

$$F^* = f \left(E (A_i^S), M_i, M_B \right) \quad 2.4.18$$

where M_i is the modulus of the inclusion i and M_B that of the matrix (note that B is implied in 2.4.18 from 2.4.4.) If the M are considered as deterministic and A_i^S lies in the bounds of 2.4.15, then extreme values of F are

$$F_{\pm} = f \left((1 \pm k) E (A_i^S), M_i, M_b \right) \quad 2.4.19$$

and
$$\frac{F^* - F_{\pm}}{F^*} = m . \quad 2.4.20$$

By retaining q in 2.4.17, increasing k then the m in 2.4.19 may be adjusted to a satisfactory value. This is accomplished by adjusting the sample value V^S .

Maximum Size

Here interest is on making the quotient 2.4.10 approach unity, or as a minimal problem by seeking to minimize ($\sigma_{\max} - \sigma_{\min}$). An indicator of the distribution of σ across the proposed meter may be obtained from an analysis of the soil structure. Such an analysis can seldom consider the three-dimensional aspects of the problem and even for linear constitutive equations only a limited number of closed solutions are available for the plane assumption. Any such solution must account for the construction sequence^{1,2} as has been demonstrated by the photo-elastic studies of Richards¹⁵. For most situations approximate solutions have to be employed where the estimates of material properties, configuration and construction sequence can be accounted for. Such a method for materials of the Markhov type has been developed by Brown and King⁵. From this type of solution an estimate of the normal stress across any line in the body can be determined. Hence an acceptable value γ in

$$\frac{2(\sigma_{\max} - \sigma_{\min})}{(\sigma_{\max} + \sigma_{\min})} = \gamma \quad 2.4.21$$

allows a maximum dimension h to be determined.

Meter Compliance

An additional matter above the previous geometric considerations concerns the stiffness of the meter in relation to the parent material. Essentially two matters have to be discussed;

- 1) The compliance of the meter relative to the soil body as a whole,
- 2) The action of the meter as a inhomogeneity in the soil.

The first part requires that an attempt be made to ensure that the meter stiffness in its design mode is much the same as the heterogeneous fill. The second part requires that the stress-concentration effect of the meter in the fill should not be any greater than that of an inclusion in the matrix.

An initial step in (1) above involves obtaining an actual expression for the modulus of the conglomerate fill rather than the form of equation 2.4.18. Here we select the lower bound of Hashin³ as an indicator of modulus. The suggestive nature of this previous statement is made because of the instabilities described in reinforced matrices by Brown and Mostaghel¹¹.

Hashin has the bulk modulus lower bound as

$$K_L^* = \frac{K_B + (2K_B + \frac{4}{3} G_B) cJ}{1 + cJ} \quad 2.4.22$$

where K_B and G_B are the matrix bulk and shear moduli,

$$J = \frac{3}{\sum_{i=1}^n A_i} \sum_{i=1}^n \frac{A_i (K_i - K_B)}{3 K_i + 4G_B} \quad 2.4.23$$

and c as described in 1.5.1 and K_i is the bulk modulus of the A_i phase.

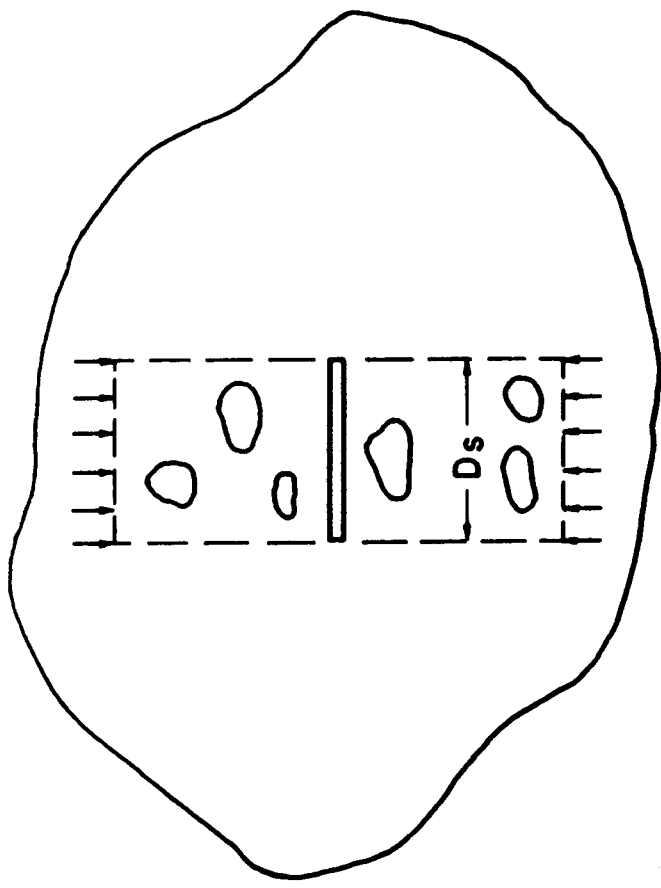
Similar expressions are possible for shear modulus.

It is now suggested that if a sample is taken from the fill material which includes the meter as in Fig. 11 then a uniaxial compression test on this sample must give a response curve of essentially same form as in a similar sample without the meter. In this way the gross effect of the meter is negligible in the fill. This means that for $\gamma = 1/4$ the response curve for the soil rock meter conglomerate should vary as $1.5 K_L^*$. A secondary effect is associated with the meter disturbing the stress pattern; this is illustrated in Fig. 12 where the meter X is on plane A-A in the body. The effect of the material stress above and on A-A is exactly the same as the reaction below and on A-A. The presence of the meter can disturb this locally as indicated in Fig. 12(b) where statical equivalence exists and when R is some radius in the meter face,

$$\int_h \sigma_{nn}^a dh = \int_h \sigma_{nn}^b dh$$

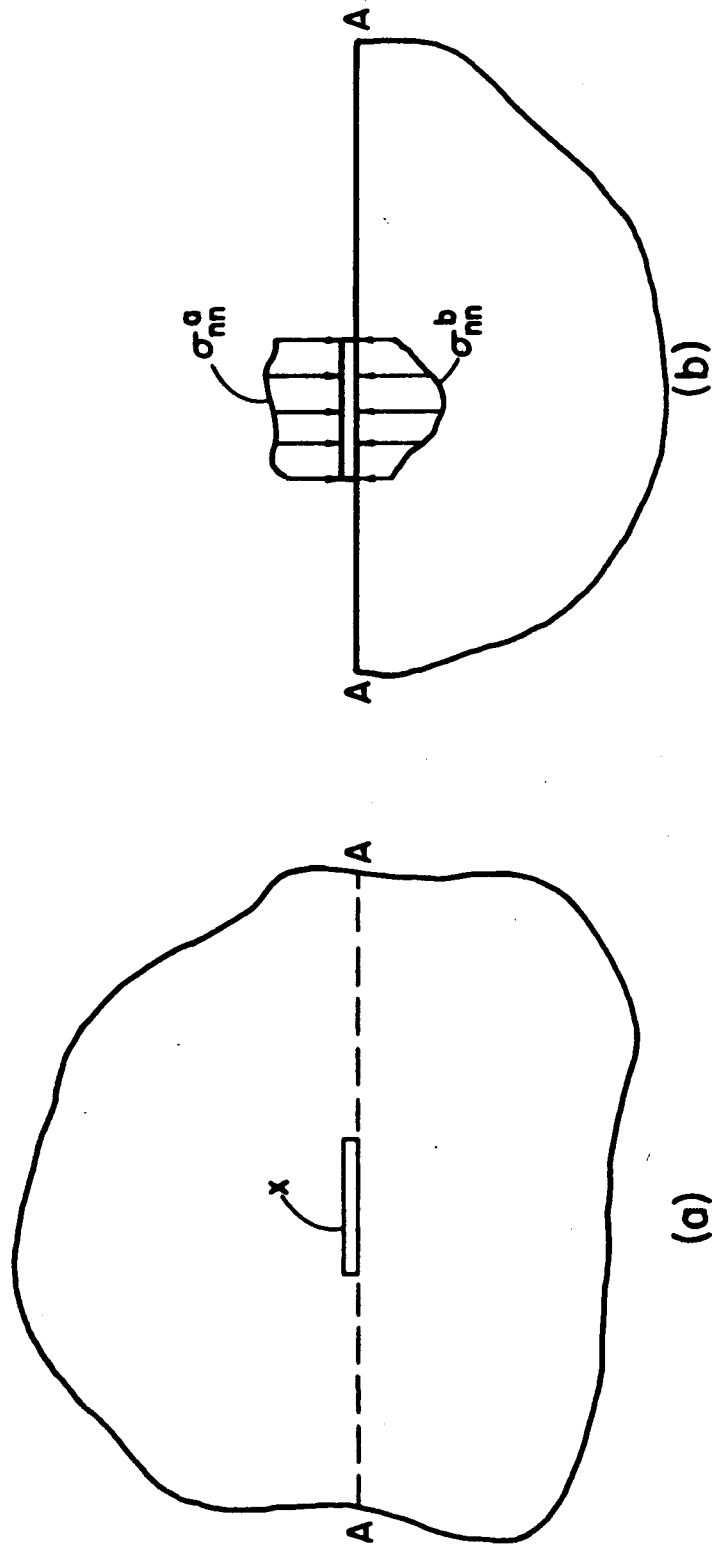
$$\int_h \sigma_{nn}^a \cdot R \cdot dh = \int_h \sigma_{nn}^b \cdot R \cdot dh \quad 2.4.24$$

However, the local distributions of σ_{nn}^a and σ_{nn}^b may differ. In particular, the σ_{nn}^a will have a very small gradient whereas σ_{nn}^b may have rapid stress gradients at the edges. One way of looking at this employs the extremes of a completely flexible meter with a traction specified boundary condition and a rigid meter with a displacement specified condition. Clearly, the actual meter provides circumstances between these extremes. Solutions for this problem by Borowicka¹⁶ indicate infinite reaction edge stresses on round plates uniformly loaded when the plates and medium are elastic. This applies for all except the completely flexible plate. In fact this edge stress will be limited to a value of the ultimate bearing capacity of the medium. The replacement of the reactive material by a deposit of cohesionless sand would alter the interface pressure distribution to be nearly parabolic¹⁷ with zero edge stresses. This results in a stress concentration



METER CONDITIONS IN FILL

FIG. 11



METER STRESS DISTRIBUTION

FIG. 12

of 1.5 (ratio of maximum reaction to the loading pressures) for uniform plate loading. To determine the acceptability of this stress concentration it is necessary to compare it with others which may occur in the rock reinforced matrix. Idealizing the material to an elastic matrix with rigid spherical inclusions, the work of Hill¹⁸ would indicate stress concentrations with a lower value of 2 and increasing as the inclusions are moved closer together. The lower value is that of Goodier¹⁹ for a single inclusion and may be further reduced for a strain softening matrix²⁰ and if the continuum admits the consideration of couple-stress²¹. However, the minimum stress concentration in the fill material would be greater than that associated with the reaction pressure under the meter as long as the meter is founded on a sand. Under this circumstance, a meter properly founded on cohesionless sand would disturb the continuum stress distribution by a smaller amount than the rock inclusions of the parent material.

Poisson Distribution Example

When the distribution of each rock type, A_i , is Poisson in the fill and independence as 2.4.3 is in effect, then the probability of $A_1^S, A_2^S, \dots, A_n^S$ in the sample V^S must be written in whole number, discrete form.

If

$$A_i^S = X_i V_i^S \quad 2.4.25$$

where X_i is the number of rocks of individual volume V_i^S making up A_i^S in V^S , and

$$E(A_i^S) = \lambda_i V_i^S \quad 2.4.26$$

then the probability of $X_1, X_2, X_3, \dots, X_n$ rocks of types 1, 2, 3...n occurring in V^S is

$$p(x_1, x_2, x_3, \dots, x_n) = \frac{(\lambda_1^{x_1} \cdot \lambda_2^{x_2} \dots \lambda_n^{x_n}) \exp. \left(- \sum_{i=1}^n \lambda_i \right)}{x_1! \cdot x_2! \cdot \dots \cdot x_n!} \quad 2.4.27$$

For each rock type the mean and variance are equal to λ_i and hence for each type the coefficient of variation is $\lambda_i^{-\frac{1}{2}}$ and 2.4.14 becomes

$$k = \frac{1}{\sqrt{\lambda_i}} \quad 2.4.28$$

The use of the Poisson distribution combined with the lower bound of Hashin as a modulus indicator allows the quantity F_{\pm} to be stated as

$$F_{\pm} = K_L^{\pm} = \frac{K_B + (2K_B + 4/3 G_B) (1 \pm k) cJ^{\pm}}{1 + (1 \pm k) cJ} \quad 2.4.29$$

and

$$F^* = K_L^* \quad 2.4.30$$

Thus, m as specified in equation 2.4.20 may be written from 2.4.22, 29, and 30.

The selection of the meter area, h , as defined by a sample diameter of D_s , results in the description of the size parameters k , q , m and γ previously developed. The acceptability of these values must be judged in the light of similar occurrences in engineering practice.

Although the previous developments for minimum meter size were predicted on known values of the moduli of matrix and all rock types, in fact, all these moduli will have a distribution the minimum coefficient of variation of which may serve as an upper acceptable value on m . It is likely that the distribution of moduli for the various phases will be normal with the resulting collection of about two-thirds of the results in a band about the mean defined by $E(1 \pm \rho)$. This suggests a value of q in 2.4.17 of about two-thirds which, with m , defines k in 2.4.15 and 16. This k is a much less restrictive parameter of homogeneity than could be obtained by purely configurational arguments alone⁸.

The maximum dimension of the meter is defined by γ in 2.4.21, which involves the normalized maximum change of stress, σ , across the meter.

This change should be no greater than that allowed in Σ in 2.4.7, the indicator for which is m as described above. Therefore, a reasonable decision of meter size rests on

$$\gamma = m < l$$

where l is the least coefficient of variation of the various phase moduli, and

$$q \approx 2/3 . \quad 2.4.32$$

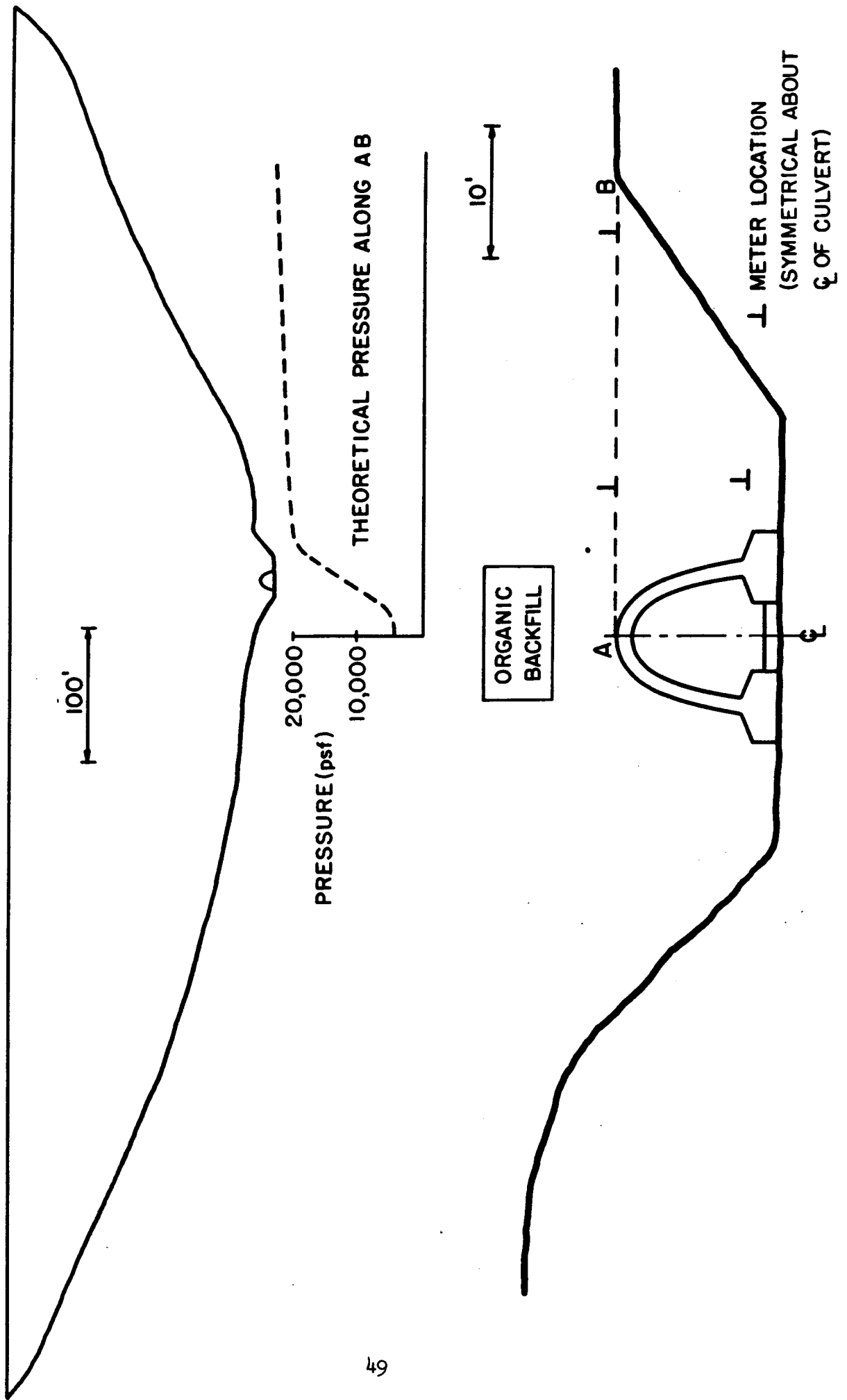
A value of l is likely to be about 0.1 from previous experience with control of concrete production and other processes.

In applying this analysis to the meter design of the San Luis relocation, the values of rock and soil properties of Section 2.2 were used. The minimum standard deviation of these materials was for the rock modulus with a value of 12%. Therefore, for $m = 0.05 < l = 0.12$ and $q = 0.683$, a minimum meter size

$$D_s = 17''$$

was obtained.

A decision on the maximum diameter was made by considering theoretical pressure plots such as shown on Fig. 13. These plots indicated the impossibility of obtaining $\gamma < m$ unless the meters were located 8' beyond the center line of the culverts. For locations closer than this distance the pressure gradient would be such that γ in 2.4.21 would take on a large and unacceptable value. For the meter positions chosen, the variation of continuum stresses, σ , as indicated by γ , over the meter of 17" diameter was small compared to m . As a second feature of maximum dimension decision the meters were founded on a 3" pack of sand which was of 30" diameter and the sand pile was eventually extended to inundate the meter in a block about 30" diameter and 12" high. In this manner the dual effects of the meter as a stress-concentration and the local pressure on the meter by a rock inclusion were minimized.



PRESSURE PLOT AT METER LOCATION

FIG 13

With such an inflexible meter as the Carlson type little can be done about altering the meter compliance to accommodate the heterogeneous fill properties. In this case a lower bound on E for the fill based on Hashin's³ work gave

$$E_{\text{fill}} = 50 \times 10^3 \text{ psi} .$$

This figure involved a change in thickness of 0.028" in a 1" meter under the full fill and was close to the average compliance of the actual device.

PART III

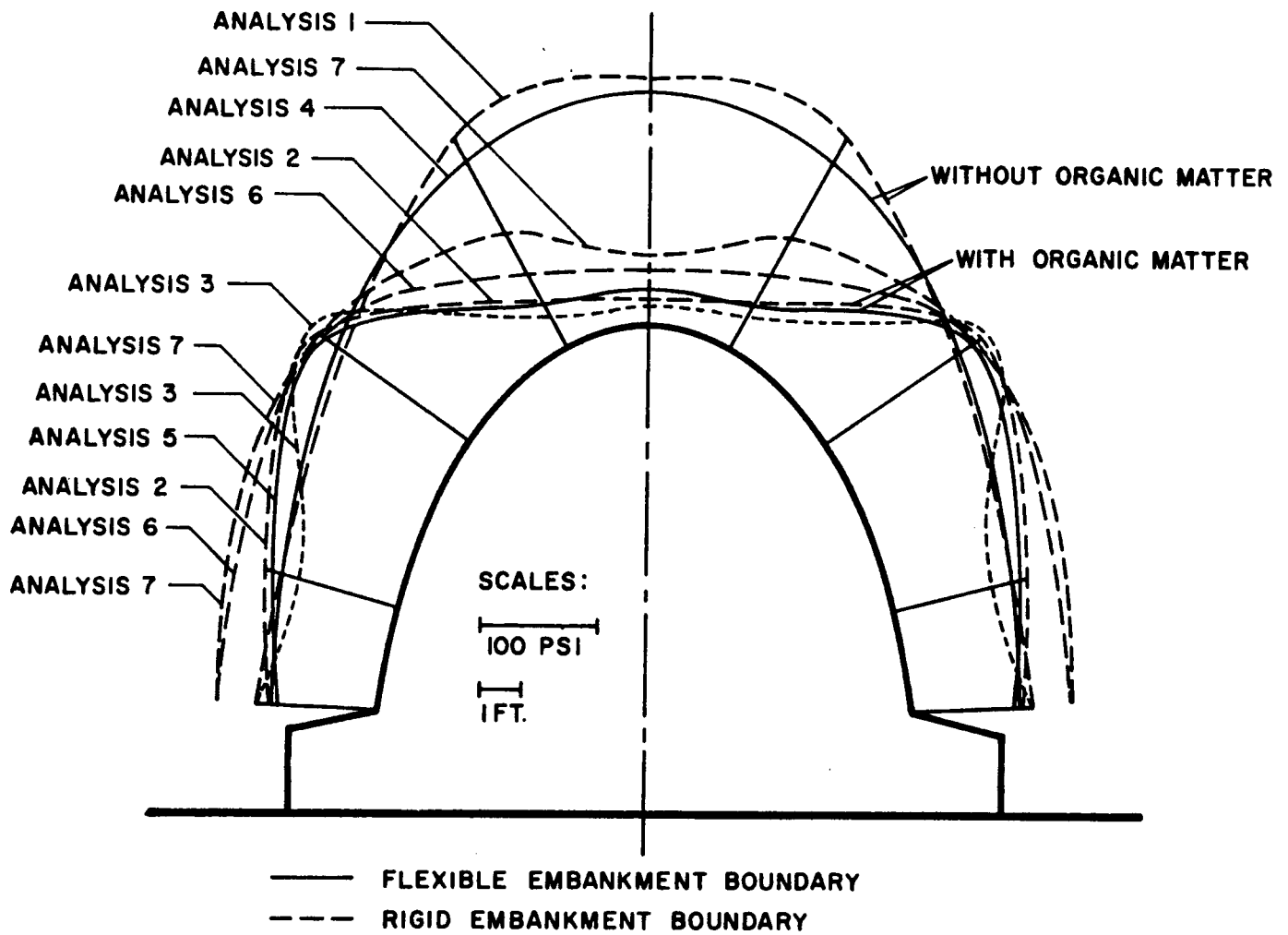
ANALYTICAL AND DESIGN CONSIDERATIONS

The discussion of analytical and design matters is based on the seven analyses of the San Luis Reservoir road relocation embankment and the pressure meter readings on that project.

3-1 Traction on the Barrel

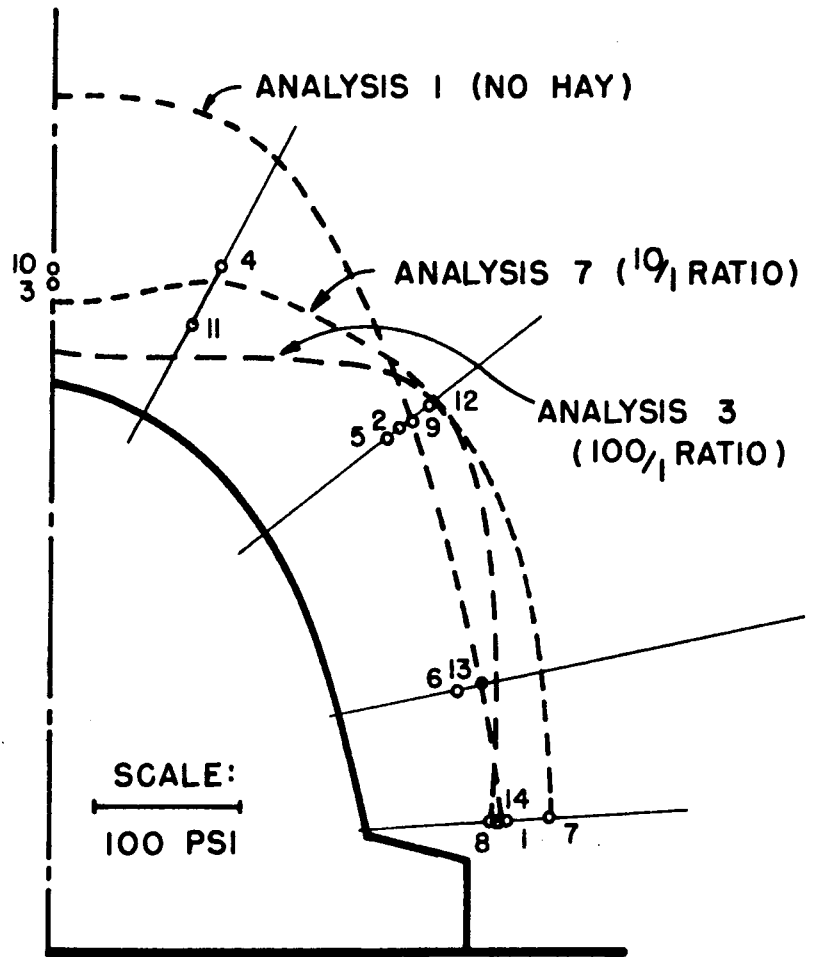
Fig. 14 shows the tractions on the barrel for the seven analyses of Table II. Fig. 15 shows the pressures measured on the barrel and the analyses associated with the rigid rock boundary. Both these figures are for conditions made the full construction depth of 200'. The effects of the history of construction, and in particular the immediate effect of the hay inclusion, are indicated in Figs. 16 and 17, where the change in pressure with fill height for two locations on the barrel are plotted. These results are at the crown and on the barrel wall; the analysis is No. 7 which appears best to represent the final pressures in Fig. 15. These figures allow consideration of the following professional questions to be made:

- 1) The extent to which the method developed is satisfactory in predicting barrel tractions.
- 2) The effect of organic inclusions.
- 3) The effect of the fill and organic material properties and their ratios.
- 4) The effect of the deformability of the earth's crust.
- 5) The effect of rotting of the organic material.



ANALYTICAL BARREL PRESSURES

FIG. 14

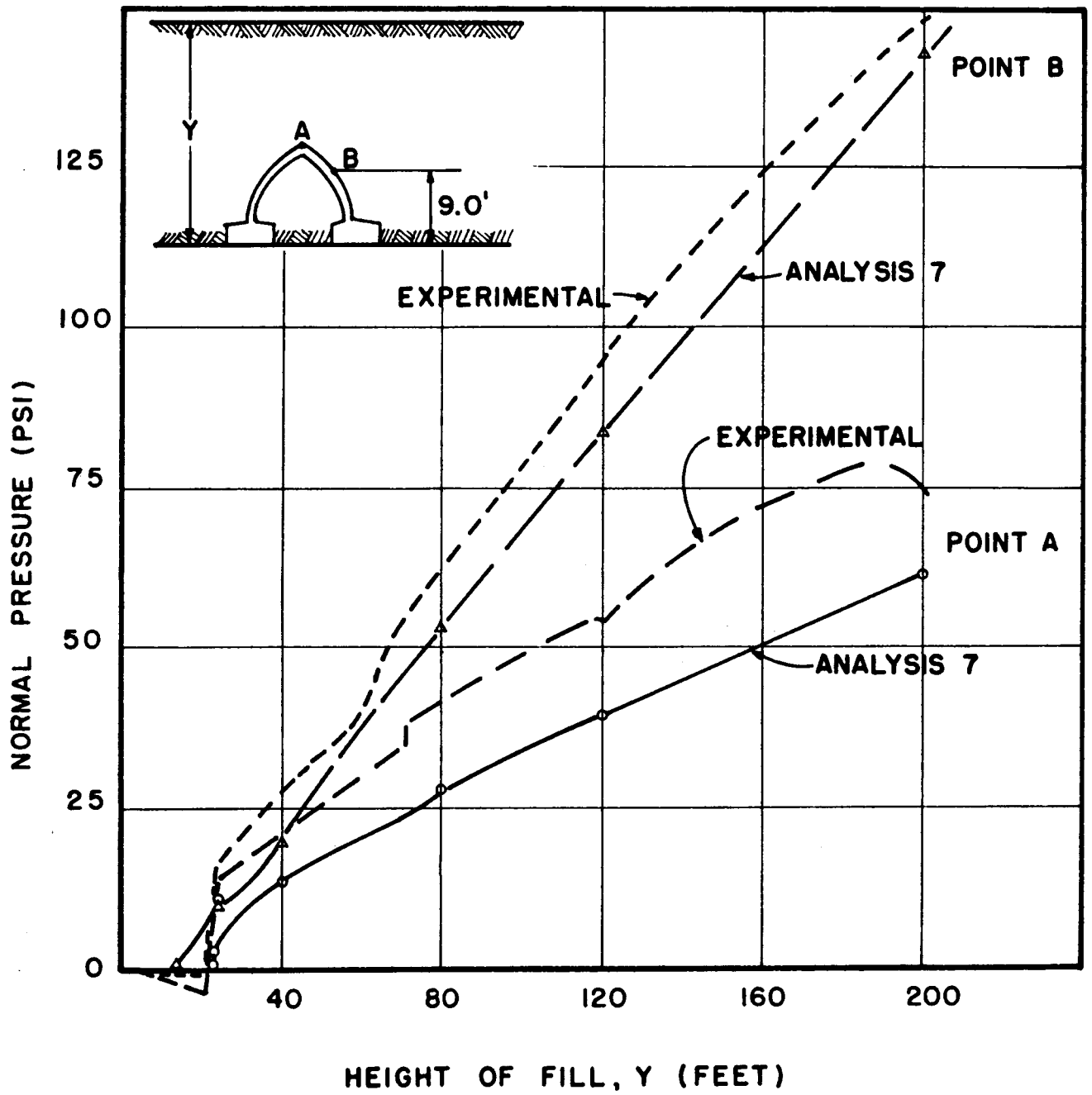


8. NORMAL PRESSURE ON METER 8 (SEE FIG. 9)

$\frac{\text{FILL}}{\text{HAY}}$ MODULUS RATIO

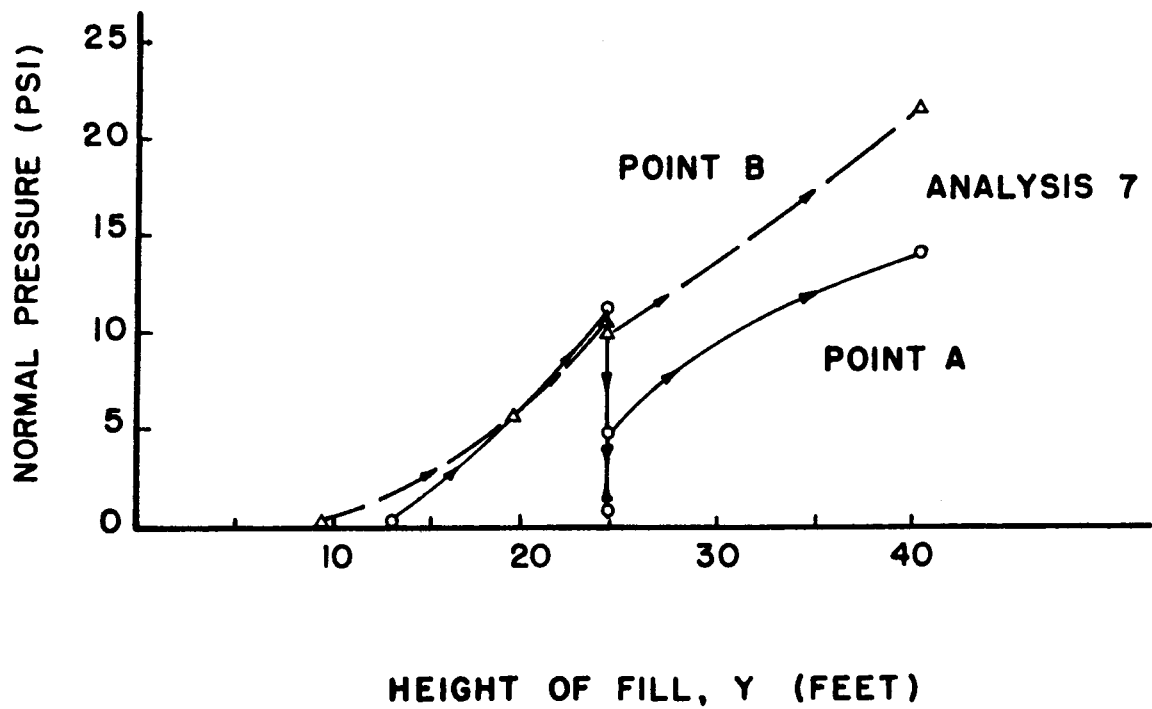
ANALYTICAL AND MEASURED BARREL PRESSURES

FIG. 15



VARIATION OF BARREL PRESSURE WITH FILL HEIGHT

FIG. 16



DETAIL OF FIG. 16

FIG. 17

The plots in Fig. 15, 16 and 17 indicate that with a proper selection of the moduli of the fill material and organic hay inclusion an accurate representation of the barrel traction distribution may be obtained. It is clear by the examination of Fig. 14 that the barrel tractions, especially at the crown region are highly sensitive to the ratio of fill:hay modulus. For no hay, when the ratio is unity, high pressures occur at the crown; these are reduced as the ratio increases. For the case of rigid boundary (Figure 4a) only this ratio is important in the analytical solution because of the homogeneous displacement boundary conditions. When the rock stiffness is included in the analysis the results will depend on the relative values of the moduli of the three materials.

The fill properties in this problem were originally ascertained from the bounds of Hashin³ but, as mentioned previously, the tests performed by Brown and Mostaghel¹¹ tended to vitiate the values of these bounds. With this in mind the results with $E_{\text{Fill}} = 1.5 \times 10^6$ psf would appear to be the most accurate representation of the fill. With regard to the hay inclusion, no definite values for a modulus were available. It would appear that a value of $E_{\text{org.}} = 0.15 \times 10^6$ psf appears most satisfactory and thus Analysis No. 7 best represents the actual fill conditions with a fill:hay modular ratio of 10.

Figs. 16 and 17 clearly show the effects of the inclusion of organic material with immediate drop of pressure and then the subsequent building up of pressure as the fill procedures continue. These characteristics are also displayed from the experimental pressure meter results.

The conclusions about the first three professional questions are that if the fill, hay and rock deformation properties, or at least their ratios, can be properly described, then the analytical model proposed can indicate accurately tractions on the barrel of the arch. Indeed, the effect of the hay inclusion is important inasmuch as it alters the characteristic shape of the pressure distribution on the barrel.

Fig. 14 indicates the effect of considering the deformability of the earth's crust. For the high rock:fill modulus ratio used (Fig. 8) the change in force distribution on the barrel is small and may be neglected in view of the confidence that can be placed in the assumptions with which the problem was commenced. When the rock modulus is closer to that of the fill the methods employed in accounting for the earth's crust effect may be utilized. It is possible that in Fig. 15 the Analysis No. 7 would have more closely matched the recorded pressures at the crown if the boundary had been non-rigid.

Over a long period of time the physical characteristics of the organic material will change and, in fact, this material will cease to exist from a structural viewpoint. This may be accounted for by clearing the hay perimeter of the stresses associated with the state of stress and displacement arrived at on pages 16 and 17, and determining the stresses and displacements (σ'_{ij} and U'_i) caused by this operation. The final states at C, namely U_i^T and σ_{ij}^T , after a long period of time will be given by

$$\begin{aligned}
 U_i^T &= U_i + U'_i \\
 \sigma_{ij}^T &= \sigma_{ij} + \sigma'_{ij}
 \end{aligned}
 \tag{3.1.1}$$

where U_i and σ_{ij} are defined by 1.2.3 and 4 together with the adjustments for the hay indicated on pages 16 and 17.

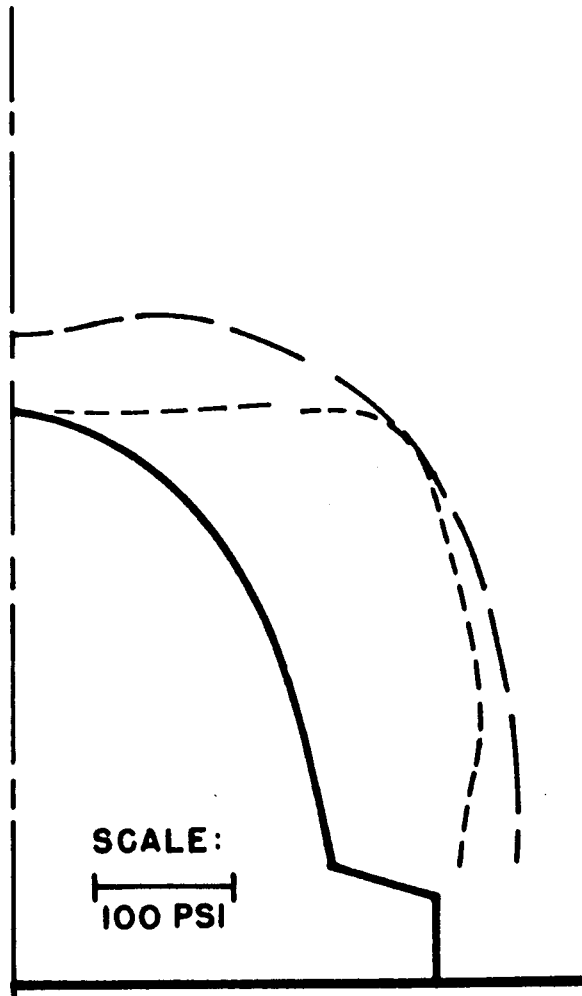
This type of operation has been carried out for Analysis No. 7. The results of σ_{nn} and σ_{nn}^T , the normal pressures on the barrel, are shown in Fig. 18.

3.2 Design Aspects of the Culvert

The design of the structural dimensions and reinforcing of a rigid culvert can only proceed with knowledge of the tractions on the surface. In this respect the analysis of this paper provides a way of obtaining this design information. However, a more important design consideration concerns arrangement of the fill to provide barrel tractions which are most satisfactory in minimizing the bending and shear action in the culvert. A state close to that of isotropic pressure would best satisfy this requirement. With accurate knowledge of the fill properties it should be possible to provide an inclusion of different material to give such axial action in the culvert. This inclusion material should be non-perishable in order that the harmful distribution of Fig. 18 is not obtained after a few years.

3.3 Fill Pressures

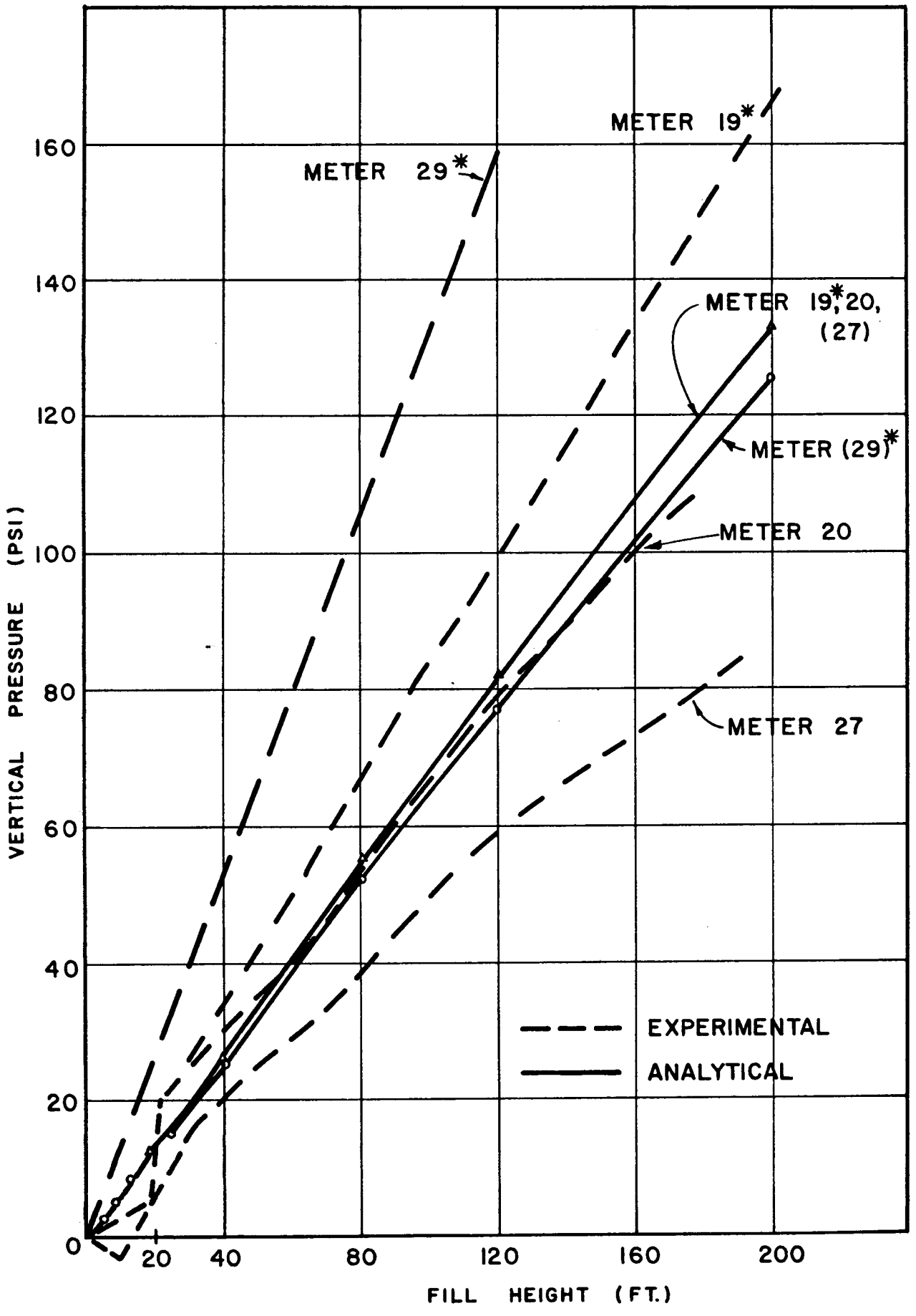
Fig. 19 gives the analytical and experimental results of fill pressures. The locations of the positions are indicated in Fig. 9. Essentially it is clear that both sets of results led to nearly linear plots which, in the theoretical case, were associated with the overburden weight. In Figs. 19 (a) and (b) the various experimental curves span the theoretical values with the triangular meters, proving to be upper, and the circular meters



——— ANALYSIS 7
 - - - ANALYSIS 7 WITH THE EFFECTS
 OF HAY ROTTING

LONG-TERM EFFECT OF HAY ROTTING

FIG. 18



SOIL PRESSURES - EXPERIMENTAL AND ANALYTICAL RESULTS

FIG. 19 (a)

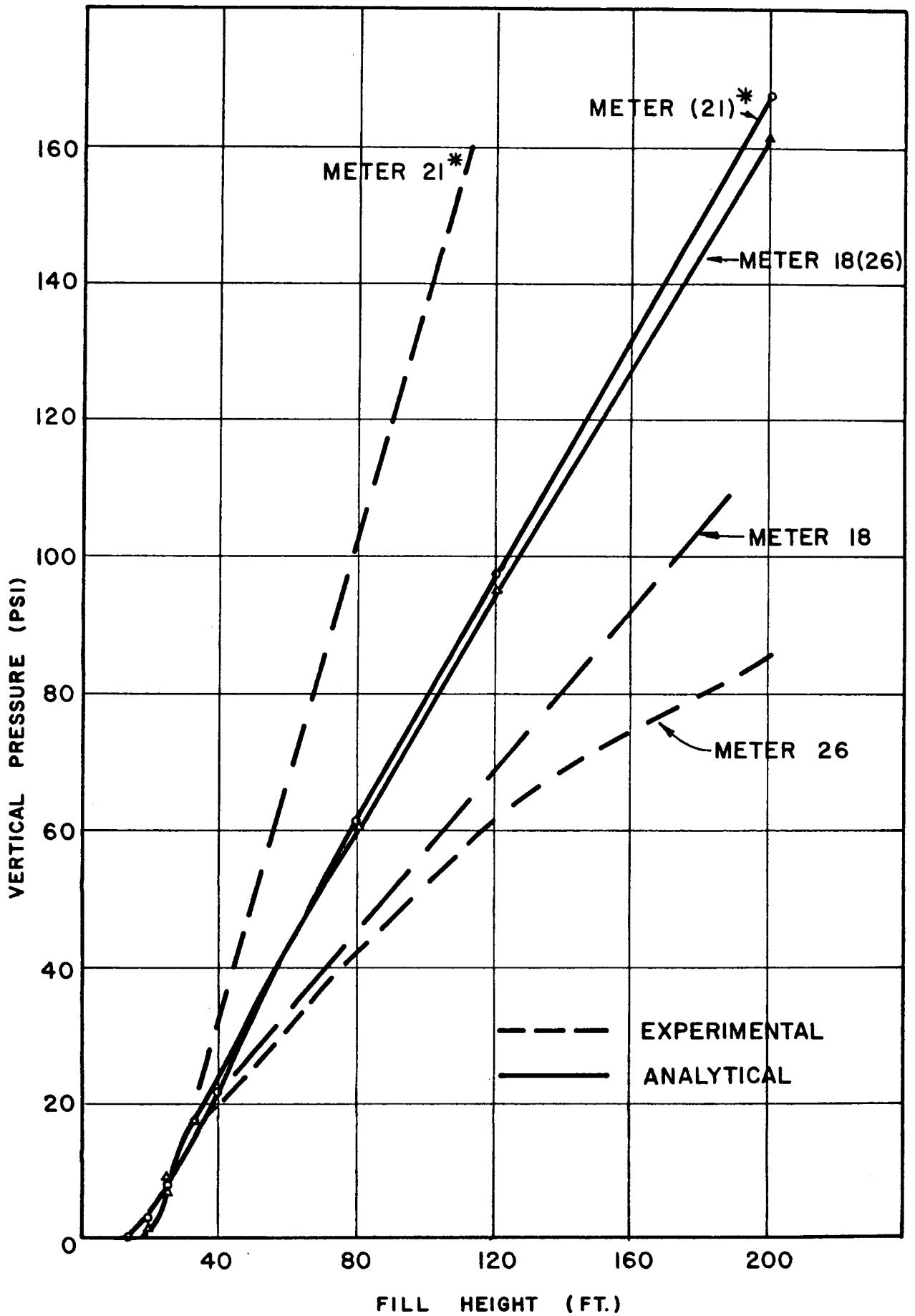


FIG. 19 (b)

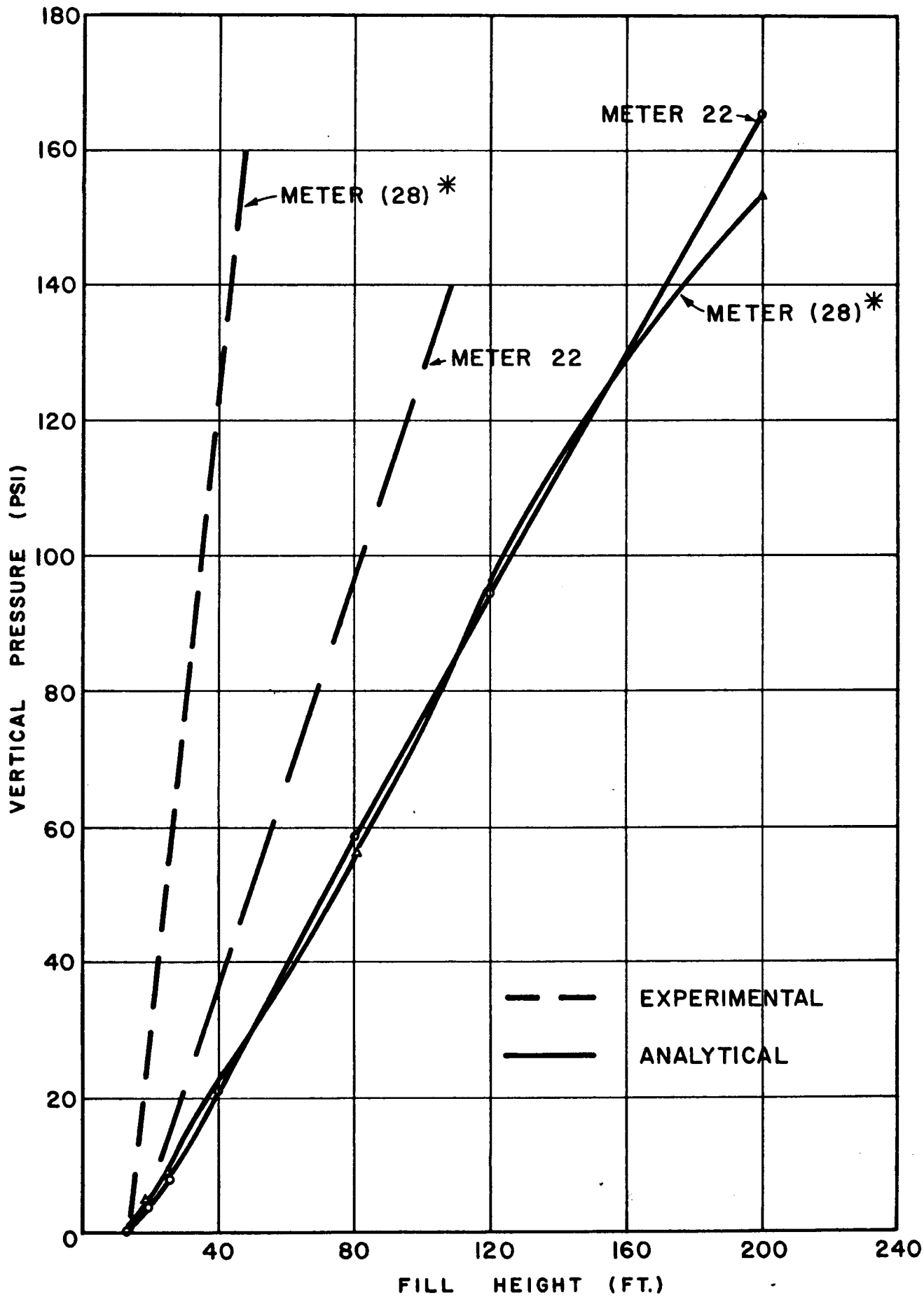


FIG. 19 (c)

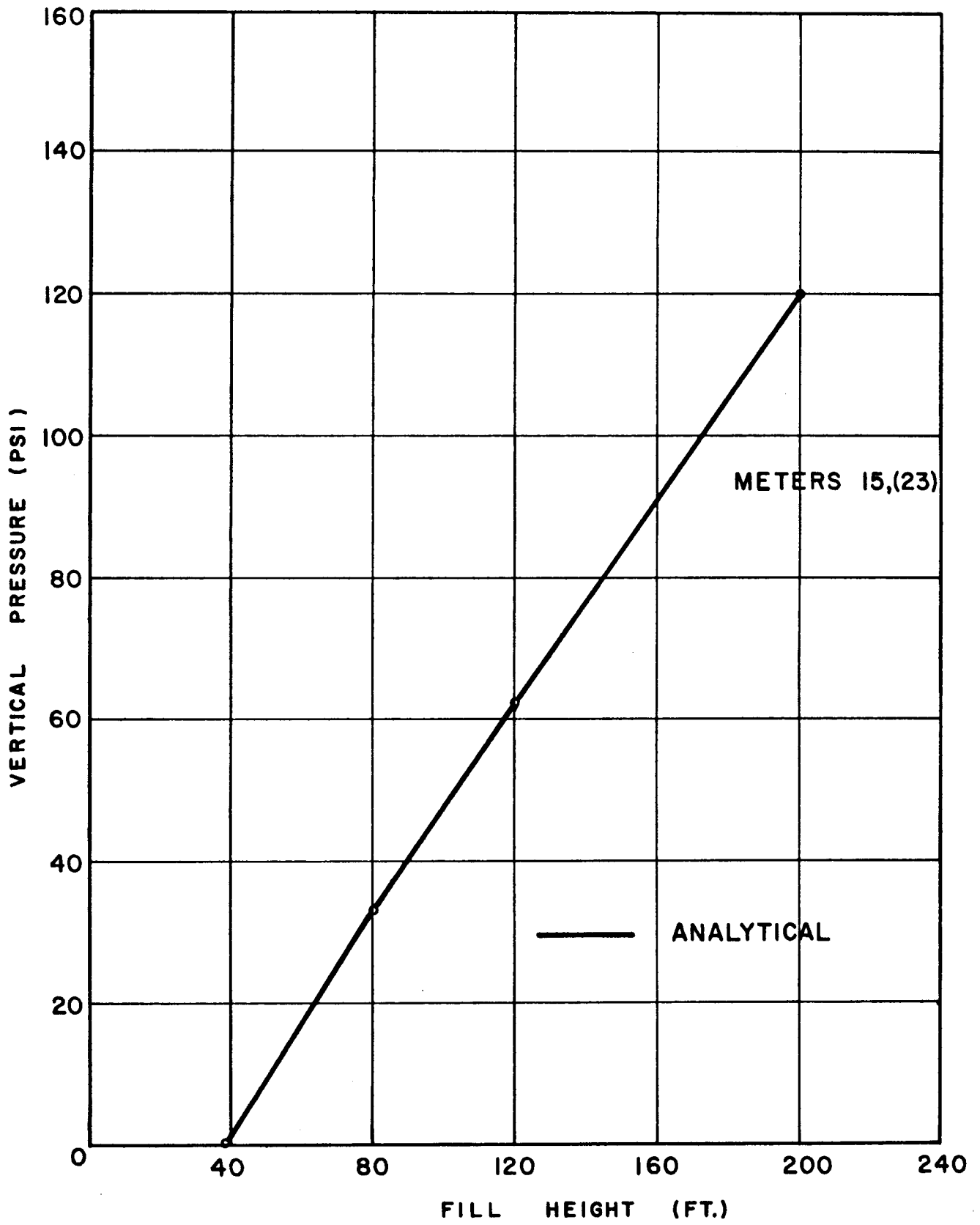


FIG. 19 (d)

to be lower bounds. Only for the meters near to the base of the culvert are the effects of the organic inclusion noticeable. The three small meter, triangular device was intended to be sensitive to local perturbations of stress across the meter; the single, 18" diameter circular meters were intended to average these local effects. The analytical results, of course, only indicate the average value of pressure over finite regions. In Fig. 19 (c) the triangular meter again gave higher pressures than the circular one, but their results are above the theoretical values. This may be caused by the close proximity of the rock boundary. Fig. 19 (d) shows the complete linearity of the theoretical readings.

From these results it could be determined that the finite-element analysis gave reasonable indications of soil pressure, which in any case, appeared to be closely associated with overburden weight regardless of the meter location. An exception to this is in the vicinity of the hard rock boundary.

3.4 Conclusions

This work has attempted to synthesize the various problems in the determination of the conditions in the fill and on the barrel of rigid culverts under high embankments. The main theoretical contributions are:

- 1) a discussion of the effective modulus of fill with large inclusions.
- 2) design methods for meters in such a fill.
- 3) analytical methods for the conditions in the fill and on the barrel, which takes into account the rock boundary and construction sequence.

This work was supported by field tests which indicated that the conditions on the barrel were well duplicated by the analysis, provided that an accurate picture of fill moduli was obtainable. In the fill itself the results of the analysis were not so well borne out.

From the professional viewpoint some important questions concerning the effects of organic inclusions were dealt with. In particular, the short and long term effect on barrel pressures were considered.

Future work could involve the consideration of culvert flexibility and the experimental investigation of the theoretical soil pressures, which appear to be essentially probable inasmuch as they vary linearly as the soil density.

References

1. Brown, C. B. and L. E. Goodman, "Gravitational Stresses in Accreted Bodies," Proc. Royal Society, London, A, Vol. 276, p. 571, 1963.
2. Goodman, L. E. and C. B. Brown, "Dead Load Stresses and the Instability of Slopes," Jnl. Soil Mech. and Fdns, Div., Proc. A.S.C.E., Vol. 89, No. SM3, p. 103, 1963.
3. Hashin, Z., "The Elastic Moduli of Heterogeneous Materials," Trans. A.S.M.E., Jnl. Applied Mechanics, Vol. 29, Ser. E, No. 1, p. 143, 1962.
4. Hashin, Z. and S. Shtrikman, "A Variational Approach to the Theory of the Elastic Behavior of Multiphase Materials," Jnl. Mech. and Phys. of Solids, Vol. 11, No. 2, p. 127, 1963.
5. Brown, C. B. and I. P. King, "Automatic Embankment Analysis: Equilibrium and Instability Conditions," Geotechnique, September 1966.
6. Kerr, A. D., "Elastic and Viscoelastic Foundation Models," Journal of Applied Mechanics, A.S.M.E., Vol. 86, p. 491, 1964.
7. King, I. P., "Finite Element Analysis of Two-Dimensional Time-Dependent Stress Problems, Structures and Materials Research Report No. 65-1, 1965, University of California, Berkeley.
8. Brown, C. B., "Minimum Volumes to Ensure Homogeneity in Certain Conglomerates." Journal of the Franklin Institute, Vol. 279, No. 3., March 1965, pp. 189-99.
9. Hill, R., "Elastic Properties of Reinforced Solids: Some Theoretical Principles," Jnl. Mech. and Physics of Solids, Vol. 11, No. 5, p. 357, 1963.
10. Paul, B., "Prediction of Elastic Constants of Multiphase Materials, Trans. A.I.M.M.P.E., Vol. 218, No. 1, p. 36, 1960.
11. Brown, C. B., and N. Mostaghel, "Modulus and Strength of Reinforced Matrices: Critical Values of Inclusion Concentration," to be published Journal of Materials, 1966.
12. Clough, R. W., "The Finite Element Method in Plane Stress Analysis," Conference Papers, 2nd Conference on Electronic Computation, A.S.C.E., p. 345, 1960.
13. Wilson, E., "Finite Element Analysis of Two-Dimensional Structures," D. Eng. Dissertation, University of California, Berkeley, 1963.
14. Lord, Kelvin, "On Homogeneous Division of Space," Proc. Royal Society, London, Vol. 55, p. 1, 1894.

15. Richards, R., Jr., "Body-Force Stresses in Wedge-Shaped Gravity Structures," Ph.D. Dissertation, Princeton University, pp. 47-51, p. 142, 1964.
16. Borowicka, H., "Influence of Rigidity of a Circular Foundation Slab on the Distribution of Pressures over the Contact Surface", Proc. Int. Conf. Soil Mech., Cambridge Mass., Vol. 2, p. 144, 1936.
17. Terzaghi, K., "Theoretical Soil Mechanics", Wiley, P. 391, 1943.
18. Hill, J. L., "The Stress Distribution in an Infinite Elastic Solid Perfectly Bonded to Two Unequal Rigid Spherical Inclusions", Special Report No. 5-50. Mathematical Studies of Composite Materials II (v). Rohm and Haas Co., p. 67, 1965.
19. Goodier, J. N., "Concentration of Stress Around Spherical and Cylindrical Inclusions and Flaws", Trans. A.S.M.E. Vol. 55, No. 7, p. 39, 1933.
20. Evans, R. J., "Physically Non-Linear Elastic Solids", Ph.D. Dissertation, University of California, Berkeley, 1965.
21. Mindlin, R. D., "Influence of Couple-Stresses on Stress Concentrations", Experimental Mechanics, Vol. 3, No. 1, p. 1, 1963.

Appendix A

$$\theta_i = \frac{b}{be - ad}$$

where

$$a = \frac{4}{5} \frac{G_o - G_i}{3K_o + 4G_o} \cdot \frac{3K_o + G_o}{G_o} (c^{7/3} - c^{5/3})$$

$$b = 4c^{7/3} \frac{6K_i + 17G_i}{3K_i + G_i} + 4(1-c^{7/3}) \frac{6K_o + 17G_o}{3K_o + G_o} u$$

$$e = \frac{G_i}{G_o} + \frac{G_o - G_i}{15K_o G_o + 20G_o^2} \left[3K_o (3 + 2c) + 4G_o (2 + 3c) \right]$$

$$d = 21u \left(\frac{1}{c^{2/3}} - 1 \right)$$

$$u = \frac{8(6K_o + 17G_o) + \frac{G_i}{G_o} (57K_i + 4G_o) (3K_o + G_o)}{35 (3K_o + 4G_o) (3K_i + G_i)}$$

$$\phi = \frac{f}{fg - ad}$$

where

$$f = 4c^{7/3} \frac{6K_i + 17G_i}{3K_i + G_i} - \frac{u}{2 (3K_o + G_o)} \left[4c^{7/3} (12K_o + 34G_o) + 57K_o + G_o \right]$$

$$g = \frac{G_i}{G_o} + \frac{9K_o + 8G_o}{5 (3K_o + 4G_o)} \left(1 - \frac{G_i}{G_o} \right) (1-c)$$

Appendix B

A BRIEF DESCRIPTION OF STRESS INTEGRATION

In the stress integration routine there are 2 options:

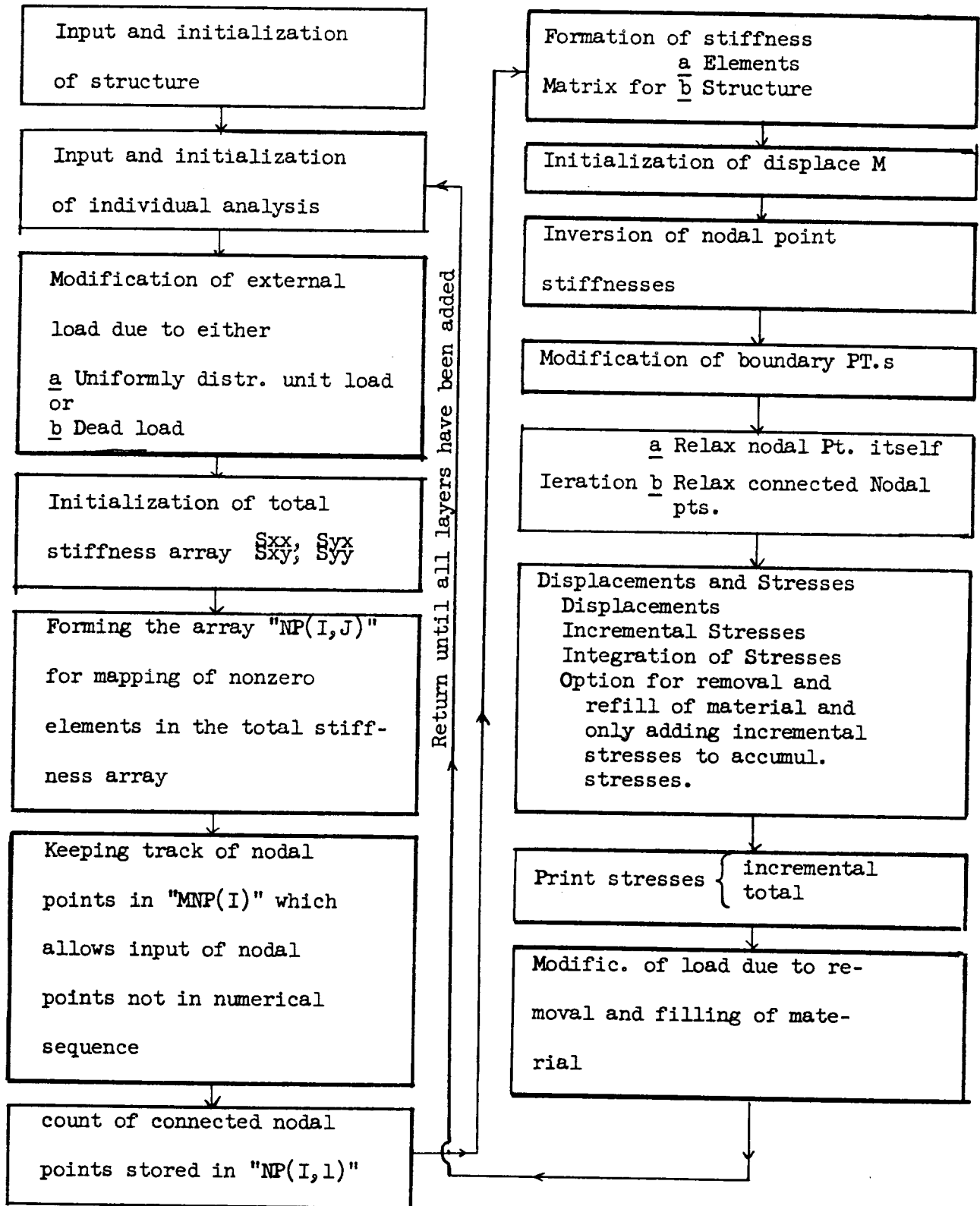
- 1) $NMNP2 = 0$ $\left\{ \begin{array}{l} \underline{a} \text{ DL is applied} \\ \underline{b} \text{ Removal or refill of material} \end{array} \right.$

- 2) $NMNP2 \neq 0$ $\left\{ \begin{array}{l} \text{Layers are added and unit} \\ \text{loads applied} \end{array} \right.$

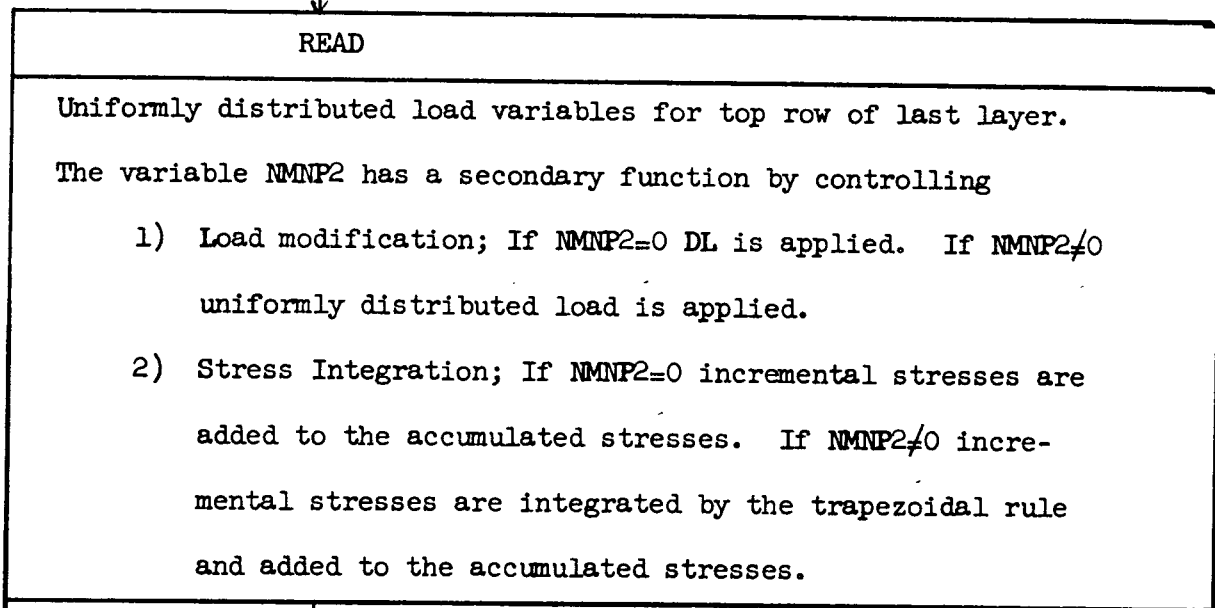
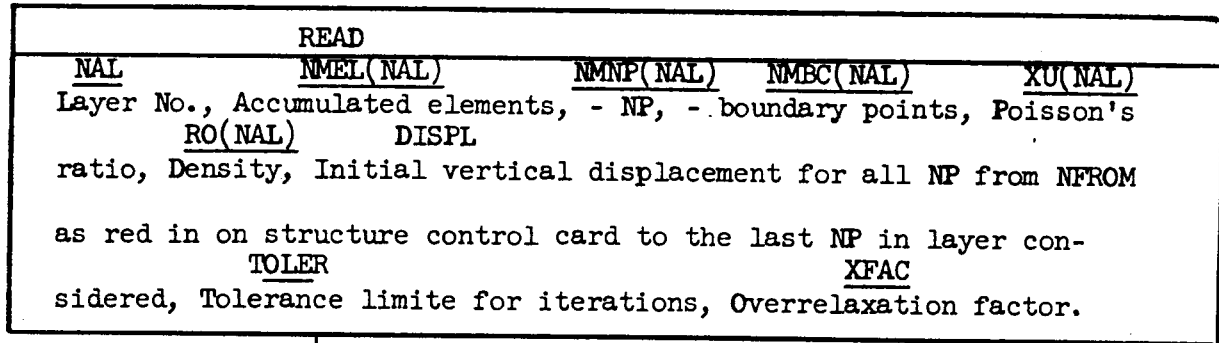
- 1) $NMNP2 = 0$ Then incremental stresses are added directly to the accumulated total of stresses existing in the elements.

- 2) $NMNP2 \neq 0$ Then incremental stresses are integrated by the trapezoidal rule for each element and added to the total existing stresses in the element.

PSIT - LAYER BY LAYER ANALYSIS



INPUT AND INITIALIZATION OF INDIVIDUAL ANALYSES - PSIT



INITIALIZATION

PRINT

CPSIT LAYER BY LAYER ANALYSIS WITH FACILITY FOR REPLACING MATERIAL

DESCRIPTION OF DATA FOR PSIT

C INPUT

C THE ELEMENTS MUST BE NUMBERED CONSECUTIVELY STARTING WITH THE
 C IN PLACE ELEMENTS AND CONTINUING ROW BY ROW

C	1ST CARD	COL.1-72	TITLE	
C	2ND CARD		PARAMETER ARRAY (1 CARD ONLY)	
C		COL.1-4	TOTAL NUMBER OF ELEMENTS	I4
C		COL.5-8	TOTAL NUMBER OF NODAL POINTS	I4
C		COL.9-12	NUMBER OF ANALYSES TO PERFORM	I4
C		COL.13-16	TOTAL NUMBER OF B. C.	I4
C		COL.17-20	FORCE UNBALANCE PRINT INTERVAL	I4
C		COL.21-24	OUTPUT INTERVAL OF FULL RESULTS	I4
C		COL.25-28	CYCLE LIMIT	I4
C		COL.29-32	FIRST NODAL POINT FOR INITIALIZATION OF DISPLACEMENTS	I4
C		COL.33-36	ELEMENT NO.-PRINT OF STRESSES FROM NEXT ELEMENT	I4
C		COL.37-38	DUMMY VARIABLE CONTROLLING OUTPUT. IF DUMMY = 0 THEN PRINT INPUT MESH ARRAYS, OTHERWISE NOT	I2
C	NEXT CARD		ELEMENT ARRAY (1 CARD FOR EACH ELEMENT)	
C		COL.1-4	ELEMENT NUMBER	I4
C		COL.5-8	NUMBER OF NODAL POINT I	I4
C		COL.9-12	NUMBER OF NODAL POINT J	I4
C		COL.13-16	NUMBER OF NODAL POINT K	I4
C		COL.17-28	MODULUS OF ELASTICITY	F12.4
C			EACH TRIANGULAR ELEMENT OF PIPE MUST HAVE NODES IN CORRECT ORDER.	
C	NEXT CARD		NODAL POINT ARRAY (1 CARD FOR EACH NODAL PT.)	
C		COL.1-4	NODAL POINT NUMBER	I4
C		COL.5-12	X-COORDINATE OF POINT	F8.1
C		COL.13-20	Y-COORDINATE OF POINT	F8.1
C		COL.21-32	X-LOAD AT POINT	F12.2
C		COL.33-44	Y-LOAD AT POINT	F12.2
C		COL.45-56	INITIAL X-DISPLACEMENT	F12.8
C		COL.57-68	INITIAL Y-DISPLACEMENT	F12.8
C	NEXT CARD		BOUNDARY ARRAY (1 CARD FOR EACH B.C.)	
C		COL.1-4	NUMBER OF BOUNDARY POINT	I4
C		COL.5-8	INDICATES RESTRAINT. (0 FOR FIXED IN BOTH DIRECTIONS. 1 FOR FIXED IN X DIRECTION. 2 FOR FIXED IN Y DIRECTION.)	I4
C		COL.9-16	SLOPE AT BOUNDARY POINT	F8.3
C	NEXT CARD		MATERIAL REPLACEMENT CARD (1 CARD ONLY)	
C		COL.1-4	NO. OF ELEMENTS TO TAKE OUT	I4
C		COL.5-8	NO. OF NODAL POINTS ALONG THE FREE EDGES OF THE EXCAVATION	I4
C		COL.9-12	ANALYSIS AT WHICH MATERIAL IS TO BE REPLACED	I4
C		COL.13-24	DENSITY OF REPLACEMENT MATERIAL	F12.4

C	COL.25-36	MODULUS OF ELASTICITY OF REPLACEMENT MATERIAL	F12.4
C	COL.37-48	ASSUMED INITIAL VERTICAL DISPLACEMENT DUE TO REMOVAL OF MATERIAL	F12.4
C	NEXT CARD	ELEMENTS TO BE REMOVED. THE ELEMENTS ARE LISTED 20 ON EACH CARD WITH A FIXED POINT FORMAT UNTIL ALL ELEMENTS WHICH ARE TO BE REMOVED ARE LISTED	2014
C	NEXT CARD	NODAL POINTS ALONG THE FREE EDGES OF THE EXCAVATION ARE LISTED 20 ON EACH CARD WITH A FIXED POINT FORMAT UNTIL ALL THE FREE NODAL POINTS ARE LISTED	2014
C	NEXT CARD	ANALYSIS CONTROL CARD (1 CARD FOR EACH ANALYSIS)	
C	COL.1-4	NUMBER OF ANALYSIS	I4
C	COL.5-8	NO. OF LAST ELEMENT IN ANALYSIS	I4
C		THE ELEMENTS OF EACH ANALYSIS MUST BE NUMBERED IN SEQUENCE	
C	COL.9-12	NO. OF NP.S IN EACH ANALYSIS	I4
C		THE NP.S NEED NOT BE NUMBERED IN SEQUENCE FOR EACH INDIVIDUAL ANALYSIS, BUT MUST BE IN SEQUENCE FOR THE COMPLETE STRUCTURE	
C	COL.13-16	NO. OF BOUNDARY POINTS IN ANALYSIS	I4
C	COL.17-24	POISSONS RATIO FOR ADDED LAYERS	F8.3
C	COL.25-34	DENSITY FOR ADDED LAYERS	F10.4
C	COL.35-44	INITIAL GUESS OF VERTICAL DISPLACEMENT	E10.4
C	COL.45-54	TOLERANCE LIMIT	F10.4
C	COL.55-62	OVER RELAXATION FACTOR	F8.4
C	NEXT CARD	LOAD APPLICATION CARD (1 CARD FOR EACH ANAL.)	
C		UNIFORMLY DISTRIBUTED LOAD IS APPLIED BETWEEN THE FIRST AND THE LAST NODAL POINT. TWO REGIONS OF DISTRIBUTED LOAD IS POSSIBLE ALONG A ROW OF NODAL POINTS AT THE SPECIFIED ELEVATION. IF THE CARD IS BLANK, GRAVITY LOAD IS APPLIED TO THE STRUCTURE.	
C	COL.1-4	FIRST NP	I4
C	COL.5-8	LAST NP.	I4
C	COL.9-12	FIRST NP	I4
C	COL.13-16	LAST NP.	I4
C	COL.17-28	ELEVATION	E12.4
C		END OF DATA CARDS.	

DIMENSION AND COMMON STATEMENTS

DIMENSION XORD(500), YORD(500), DSX(500), DSY(500), SIGXXT(800), 1MNP(500), XLOAD(500), YLOAD(500), NP(500,8), NPI(800), NPJ(800), 2NPK(800), NMEL(100), NMNP(100), NMRC(100), FT(800), XU(100), RO(100), 3SLOPE(100), NPB(100), NFIX(100), SXX(2000), SXY(2000), SYX(2000), 4SYY(2000), FRX(500), FRY(500), ELEV(100), SIGXX(800), SIGXY(800), 5SIGYY(800), LM(3), A(6,6), B(6,6), S(6,6), SIGYYT(800), SIGXYT(800) 6, NELOUT(100), NPFREE(50), SIG(3)
COMMON SXX, SXY, SYX, SYY, SIGXX, SIGXY, SIGYY, NPI, NPJ, NPK, XORD, YORD

C
C
C

FORMAT STATEMENTS

1 FORMAT (72H1 BCD INFORMATION
1)
2 FORMAT (9I4,I2)
3 FORMAT (31H0TOTAL NUMBER OF ELEMENTS =I14/)
4 FORMAT (31H TOTAL NUMBER OF NODAL POINTS =I14/)
5 FORMAT (31H NO. OF ANALYSES TO PERFORM =I14/)
6 FORMAT (31H CYCLE PRINT INTERVAL =I14/)
7 FORMAT (31H OUTPUT INTERVAL OF RESULTS =I14/)
8 FORMAT (31H CYCLE LIMIT =I14/)
9 FORMAT (22H TOLERANCE LIMIT =E9.3)
10 FORMAT (22H RELAXATION FACTOR =F6.3)
11 FORMAT (27H1EL. I J K F)
12 FORMAT (4I4,E12.4)
13 FORMAT (80H1 NP X-ORD Y-ORD X-LOAD Y-LOA
1D X-DISP Y-DISP)
14 FORMAT (1I4,2F8.1,2F12.2,2F12.8)
15 FORMAT (40H0NO. OF TERMS IN TOTAL STIFFNESS ARRAYS =I6)
16 FORMAT (43H1RESULTS FOR ELEMENTS IN PLACE-ANALYSIS NO. I4/22H0NO. O
1F ELEMENTS =I4/22H NO. OF NODAL POINTS =I4/22H NO. OF B.C.
2 =I4)
17 FORMAT (3I4,3F12.4)
18 FORMAT (4I4,F8.3,3E10.4,F8.4)
19 FORMAT (31H TOTAL NUMBER OF B.C. =I14/)
20 FORMAT (1I8,4F12.1,2F12.8)
21 FORMAT (2I4,1F8.3)
22 FORMAT (20H0BOUNDARY CONDITIONS)
23 FORMAT (32H0 CYCLE FORCE UNBALANCE)
24 FORMAT (1I12,1E20.6)
25 FORMAT (42H0NODAL POINT X-DISPLACEMENT Y-DISPLACEMENT)
26 FORMAT (1I12,2F15.6)
27 FORMAT (120H1 ELEMENT X-STRESS Y-STRESS XY-STRESS
1 MAX.STRESS MIN.STRESS MAX.SHFAR DIRECTION)
28 FORMAT (1I10,3F15.4,5X,4F15.2)
29 FORMAT (25H1RESULTS FOR ANALYSIS NO. I4/22H0NO. OF ELEMENTS =
I14 /22H NO. OF NODAL POINTS =I4/ 22H NO. OF B.C. =I4)
30 FORMAT (1H1)
31 FORMAT (37H-MODIFIED VERTICAL LOADS AT ELEVATION F8.2/13H NP. YL
LOAD)
32 FORMAT (15H-TOTAL STRESSES /56H ELEMENT X-STRESS Y-S
1TRESS XY-STRESS)
33 FORMAT (22H POISSONS RATIO =F6.3/22H DENSITY =E9.
13)
34 FORMAT (22H1ANALYSIS OF THE FIRST 13,8H LAYERS)
35 FORMAT (39H MATERIAL IS REMOVED AND LOADS MODIFIED /20H NP. XLOA
1D YLOAD)
36 FORMAT (36H PIT IS FILLED WITH ORGANIC MATERIAL/9H DENSITY=E12.4/
19H F =F12.4)
37 FORMAT (20I4)
38 FORMAT (I8,2F12.4)
39 FORMAT (32H- NP. XLOAD YLOAD)
41 FORMAT (E12.4)
711 FORMAT (32H0ZERO OR NEGATIVE AREA, FL. NO.=I14)
712 FORMAT (36H0MORE THAN 7 POINTS CONNECTED TO NP. I4)

C
C
C

READ AND PRINT INPUT DATA

```

PRINT 30
READ 1
PRINT 1
READ 2,NUMELT,NUMNPT,NANAL ,NUMBCT,NCPIN,NOPIN,NCYCM,NFROM,
1 NBLOCK,T1
PRINT 3,NUMELT
PRINT 4,NUMNPT
PRINT 5,NANAL
PRINT 19,NUMBCT
PRINT 6,NCPIN
PRINT 7,NOPIN
PRINT 8,NCYCM
READ 12,(N,NPI(N),NPJ(N),NPK(N),FT(N),
N=1,NUMFLT)
111 CONTINUE
READ 14,(M,XORD(M),YORD(M),XLOAD(M),YLOAD(M),DSX(M),DSY(M),M=1,NUM
1NPT)
READ 21,(NPB(L),NFIX(L),SLOPE(L),L=1,NUMBCT)
IF (T1) 105,100,105
100 PRINT 11
PRINT 12,(N,NPI(N),NPJ(N),NPK(N),FT(N),
N=1,NUMFLT)
PRINT 13
PRINT 20,(M,XORD(M),YORD(M),XLOAD(M),YLOAD(M),DSX(M),DSY(M),M=1,NU
1MNPT)
PRINT 22
PRINT 21,(NPB(L),NFIX(L),SLOPE(L),L=1,NUMBCT)
105 READ 17,NOUT,NFREE,NT0,ROR,ETORG,DORG
PRINT 17,NOUT,NFREE,NT0,ROR,ETORG,DORG
READ 37,(NELOUT(I),I=1,NOUT)
PRINT 37,(NELOUT(I),I=1,NOUT)
READ 37,(NPFREE(I),I=1,NFREE)
PRINT 37,(NPFREE(I),I=1,NFREE)
C
C INITIALIZATION OF ANALYSIS OF COMPLETE STRUCTURE
C
110 NCTAG= 8
NDIM=2000
IFLAG=0
NAL=0
NNN=0
NID=0
C
C INITIALIZATION OF INDIVIDUAL ANALYSIS
C
120 READ 18 ,(NAL),(NMEL(NAL),NMNP(NAL),NMBC(NAL),XU(NAL),RO(NAL),DTSP
1L,TOLER,XFAC)
READ 12,NMNP1,NMNP2,NMNP3,NMNP4,ELFV(NAL)
NUMFL=NMEL(NAL)
NUMNP=NMNP(NAL)
NUMBC=NMBC(NAL)
IF (NAL-1) 125,122,125
122 NNUMFL=1
PRINT 16,NAL,NUMEL,NUMNP,NUMBC
GO TO 127
125 NNUMEL=NMEL(NAL-1)+1
PRINT 29,NAL,NUMEL,NUMNP,NUMBC
127 PRINT 10,XFAC
PRINT 13,XU(NAL),RO(NAL)
PRINT 9,TOLER
IF (NMNP2) 145,145,139

```



```

C
C   UNIT LOAD MODIFICATION
C
139 PRINT 31 ,ELEV(NAL)
143 DO 142 N=NMNP1,NMNP2
    IF (N-NMNP2 ) 140,141,141
140 UNITL=ABSF((XORD(N+1)-XORD(N)) /2.0)
    YLOAD(N)=YLOAD(N)-UNITL
    YLOAD(N+1)=YLOAD(N+1)-UNITL
141 PRINT 14,N,YLOAD(N)
142 CONTINUE
    IF (NMNP3) 145,145,144
144 NMNP1=NMNP3
    NMNP2=NMNP4
    NMNP3=0
    GO TO 143
145 IF (NMNP2) 146,146,129
C
C   DEAD LOAD MODIFICATION
C
146 NFEL=NUMEL
    NLEL=NUMEL
    RORG=RO(NAL)
147 DO 161 M=NFEL,NLEL
    IF (NMNP2) 156,157,156
156 N=NELOUT(M)
    GO TO 158
157 N=M
158 I=NPI(N)
    J=NPJ(N)
    K=NPK(N)
    AJ=XORD(J)-XORD(I)
    AK=XORD(K)-XORD(I)
    BJ=YORD(J)-YORD(I)
    BK=YORD(K)-YORD(I)
    AREA=(AJ*BK-AK*BJ)/2.0
159 DL=AREA*RORG /3.0
160 YLOAD(I)=YLOAD(I)-DL
    YLOAD(J)=YLOAD(J)-DL
161 YLOAD(K)=YLOAD(K)-DL
    PRINT 39
    PRINT 38,(M,XLOAD(M),YLOAD(M),M=1,NUMNP)
129 NCYCLE=0
    NUMPT=NCPIN
    NUMOPT=NOPIN
    DO 130 L=1,NDIM
    SXX(L)=0.0
    SXY(L)=0.0
    SYX(L)=0.0
130 SYX(L)=0.0
C
C
C   THE TAG ARRAY FOR MAPPING OF TOTAL STIFNESSES IS FORMED
C
162 DO 170 N=1,NUMEL
    LM(1)=NPI(N)
    LM(2)=NPJ(N)
    LM(3)=NPK(N)
    DO 170 II=1,3

```

```

MS=LM(II)
NP(MS,1)=MS
DO 170 JJ=1,2
C
  IF (MS-LM(JJ)) 165,170,170
165 DO 168 LS=2,NCTAG
166 IF (NP(MS,LS)-LM(JJ)) 167,170,167
167 IF (NP(MS,LS)) 163,169,163
163 IF (LS-NCTAG) 168,164,164
164 IFLAG=1
  PRINT 712,MS
168 CONTINUE
C
C IF NP IS ZERO, STORE LM(JJ)
169 NP(MS,LS)=LM(JJ)
170 CONTINUE
  IF (IFLAG) 442,153,442
C
C CONSECUTIVE NUMBERING OF NODAL POINT LABELLING ARRAY
C
153 L=0
  DO 155 N=1,NUMNPT
  IF (NP(N,1)) 155,155,154
154 L=L+1
  MNP(L)=NP(N,1)
155 CONTINUE
  MNP(NUMNP+1)=MNP(NUMNP)+1
C
C COUNTING ADJACENT NODAL POINTS, THE COUNT IS STORED
C IN THE FIRST COLUMN OF THE TAG ARRAY
C
NP(1,1)=1
DO 175 M=1,NUMNP
  I=MNP(M)
  IN=MNP(M+1)
  N=1
171 N=N+1
  IF (NP(I,N)) 174,174,172
172 IF (N-NCTAG) 171,173,173
173 NP(IN,1)=N+NP(1,1)
  GO TO 175
174 NP(IN,1)=N+NP(1,1)-1
175 CONTINUE
C
C PRINTOUT OF NUMBER OF CONNECTED NODAL POINTS. THIS SHOULD EQUAL THE
C NUMBER OF TERMS IN EACH OF THE TOTAL STIFFNESS ARRAYS AND NOT
C EXCEED NDIM.
C
  N=MNP(NUMNP)
  NUMTOT=NP(N,1)
  PRINT 15,NUMTOT
  IF (NDIM-NUMTOT) 442,176,176
C
C FORMATION OF STIFFNESS ARRAY
C
176 M=0
178 M=M+1
  NLSI=NMEL(M)
  IF (M -1) 180,179,180

```

```

179 NFSI=1
    GO TO 181
180 NFSI=NMEL(M-1)+1
181 DO 199 N=NFSI,NLSI
    I=NPI(N)
    J=NPJ(N)
    K=NPK(N)
    AJ=XORD(J)-XORD(I)
    AK=XORD(K)-XORD(I)
    BJ=YORD(J)-YORD(I)
    BK=YORD(K)-YORD(I)
    AREA=(AJ*BK-AK*BJ)/2.0
C
    PRINT OF ERRORS IN INPUT DATA
    IF (AREA) 701,701,700
700 IF (IFLAG) 702,702,199
701 PRINT 711,N
    IFLAG=1
    GO TO 199
702 COMM=0.25*EI(N)/((1.-XU(M)**2)*AREA)
    A(1,1)=BJ-BK
    A(1,2)=0.0
    A(1,3)=BK
    A(1,4)=0.0
    A(1,5)=-BJ
    A(1,6)=0.0
    A(2,1)=0.0
    A(2,2)=AK-AJ
    A(2,3)=0.0
    A(2,4)=-AK
    A(2,5)=0.0
    A(2,6)=AJ
    A(3,1)=AK-AJ
    A(3,2)=BJ-BK
    A(3,3)=-AK
    A(3,4)=BK
    A(3,5)=AJ
    A(3,6)=-BJ
    IF (NFSI-NLSI) 703,520,703
703 B(1,1)=COMM
    B(1,2)=COMM*XU(M)
    B(1,3)=0.0
    B(2,1)=COMM*XJ(M)
    B(2,2)=COMM
    B(2,3)=0.0
    B(3,1)=0.0
    B(3,2)=0.0
    B(3,3)=COMM*(1.-XU(M))*0.5
C
    DO 182 JJ=1,6
    DO 182 II=1,3
    S(II,JJ)=0.0
    DO 182 KK=1,3
182 S(II,JJ)=S(II,JJ)+B(II,KK)*A(KK,JJ)
    DO 183 JJ=1,6
    DO 183 II=1,3
183 R(JJ,II)=S(II,JJ)
    DO 184 JJ=1,6
    DO 184 II=1,6

```

```

S(II,JJ)=0.0
DO 184 KK=1,3
184 S(II,JJ)=S(II,JJ)+B(II,KK)*A(KK,JJ)
C
C   SEARCHING FOR AND STORING NONZERO TERMS OF THE
C   TOTAL STIFNESS ARRAY
C
LM(I)=NP1(N)
LM(2)=NPJ(N)
LM(3)=NPK(N)
DO 198 II=1,3
KS=LM(II)
DO 198 JJ=1,3
NS=NP(KS,1)
LS=LM(JJ)
IF (KS-LS) 186,195,198
186 DO 188 MS=2,NCIAG
187 NS=NS+1
IF (NP(KS,MS)-LS) 188,195,188
188 CONTINUE
195 SXX(NS)=SXX(NS)+S(2*II-1,2*JJ-1)
SXY(NS)=SXY(NS)+S(2*II-1,2*JJ )
SYX(NS)=SYX(NS)+S(2*II ,2*JJ-1)
SYY(NS)=SYY(NS)+S(2*II ,2*JJ )
198 CONTINUE
199 CONTINUE
IF (M-NAL) 178,200,200
200 CONTINUE
IF (IFLAG) 442,201,442
C
C   INITIALIZATION OF DISPLACEMENTS
C
201 DO 205 I=NFROM,NUMNP
N=MNP(I)
IF (NID-1) 204,202,203
202 DSY(N)=DORG
GO TO 205
203 DSY(N)=-DSY(N)
GO TO 205
204 DSY(N)=DISPL
205 DSX(N)=0.0
C
C   INVERSION OF NODAL POINT STIFNESSES
C
DO 210 I=1,NUMNP
M=MNP(I)
N=NP( M,1)
COMM =SXX(N)*SYY(N)-SXY(N)*SYX(N)
IF (COMM) 208,209,208
208 TEMP=SYY(N)/COMM
SYY(N)=SXX(N)/COMM
SXX(N)=TEMP
SXY(N)=-SXY(N)/COMM
SYX(N)=-SYX(N)/COMM
209 FRX(M)=XLOAD(M)
210 FRY(M)=YLOAD(M)
C
C   MODIFICATION OF BOUNDARY FLEXIBILITIES
C

```

```

DO 240 L=1,NUMBC
M=NPB(L)
N=XABSF(NP(M,1))
NP(M,1)=-NP(M,1)
IF(NFIX(L)-1) 225,220,215
215 C=(SXX(N )*SLOPE(L)-SXY(N ))/(SYX(N )*SLOPE(L)-SYY(N ))
R=1.-C*SLOPE(L)
SXX(N )=(SXX(N )-C*SYX(N ))/R
SXY(N )=(SXY(N )-C*SYY(N ))/R
SYX(N )=SXX(N )*SLOPE(L)
SYY(N )=SXY(N )*SLOPE(L)
DSY(M)=0.0
GO TO 240
220 SYY(N )=SYY(N )-SYX(N )*SXY(N )/SXX(N )
DSX(M)=0.0
GO TO 230
225 SYY(N )=0.0
DSY(M)=0.0
DSX(M)=0.0
230 SXX(N )=0.0
235 SXY(N )=0.0
SYX(N )=0.0
240 CONTINUE
C
C ITERATION OF NODAL POINT DISPLACEMENTS
C
243 PRINT 23
245 SUM=0.0
DO 290 I=1,NUMNP
N=MNP(I)
NN=MNP(I+1)
C
C NODAL POINT N IS RELAXED
NM=XABSF(NP(N,1))
IF (SXX(NM)+SYY(NM)) 249,290,249
249 NAP=XABSF(NP(NN ,1))-XABSF(NP(N,1))-1
IF (NAP) 260,260,250
250 DO 255 LL=1,NAP
NB=NP(N,LL+1 )
M =LL+NM
FRX(N)=FRX(N)-SXX(M)*DSX(NB)- SXY(M)*DSY(NB)
255 FRY(N)=FRY(N)-SYX(M)*DSX(NB)- SYY(M)*DSY(NB)
260 DX=SXX(NM)*FRX(N)-DSX(N)+SXY(NM)*FRY(N)
DY=SYX(NM)*FRX(N)-DSY(N)+SYY(NM)*FRY(N)
DSX(N) =DSX(N) +XFAC*DX
DSY(N) =DSY(N) +XFAC*DY
IF (NP(N,1)) 265,262,262
262 SUM=SUM+ABSF(DX/SXX(NM))+ABSF(DY/SYY(NM))
C
C NODAL POINTS CONNECTED TO NODAL POINT N ARE RELAXED
IF (NAP) 280,280,265
265 DO 275 LL=1,NAP
NB=NP(N,LL+1)
M=LL+NM
FRX(NB)= -SXX(M)*DSX(N) - SYX(M)*DSY(N )+FRX(NB)
275 FRY(NB)= -SXY(M)*DSX(N) - SYY(M)*DSY(N )+FRY(NB)
280 FRX(N)=XLOAD(N)
FRY(N)=YLOAD(N)
290 CONTINUE

```

```

C
C   CYCLF COUNT AND PRINT CHECK
C
      NCHECK=0
      NCYCLE=NCYCLE +1
      IF (NCYCLE-NUMPT) 301,300,300
300  NUMPT=NUMPT+NCPIN
      PRINT 24,NCYCLE,SUM
301  IF (SUM-TOLFR) 305,305,302
302  IF (NCYCM-NCYCLE) 305,305,303
303  NCHECK=1
      IF (NCYCLE-NUMOPT) 245,304,304
304  NUMOPT=NUMOPT+NOPIIN
C
C   PRINT OF DISPLACEMENTS AND STRESSES
C
305  PRINT 25
      DO 307 I=1,NUMNP
      M=MNP(I)
307  PRINT 26,M,DSX(M),DSY(M)
      PRINT 27
      DO 421 M=1,NAL
      NLST=NMEL(M)
      IF (M -1) 311,310,311
310  NFST=1+NBLOCK
      GO TO 312
311  NFST=NMEL(M-1)+1
312  DO 421 N=NFST,NLST
      I=NPI(N)
      J=NPJ(N)
      K=NPK(N)
      AJ=XORD(J)-XORD(I)
      AK=XORD(K)-XORD(I)
      BJ=YORD(J)-YORD(I)
      BK=YORD(K)-YORD(I)
      EPX=(BJ-BK)*DSX(I)+BK*DSX(J)-BJ*DSX(K)
      EPY=(AK-AJ)*DSY(I)-AK*DSY(J)+AJ*DSY(K)
      GAM=(AK-AJ)*DSX(I)-AK*DSX(J)+AJ*DSX(K)+
      (BJ-BK)*DSY(I)+BK*DSY(J)-BJ
      *DSY(K)
      COMM=ET(N)/((1.-XU(M)**2)*(AJ*BK-AK*BJ))
      X=COMM*(EPX+XU(M)*FPY)
      Y=COMM*(EPY+XU(M)*EPX)
      XY=COMM*GAM*(1.-XU(M))*0.5
      IF (NCHECK) 321,317,321
317  IF (NMNP2) 319,328,319
319  IF (NNN-1) 320,328,328
320  IF (NAL-M) 322,322,323
322  CG=(YORD(I)+YORD(J)+YORD(K))/3.0
      SIGYY(N)=-1.0
      GO TO 324
323  CG=ELEV(NAL-1)
324  TMUL=(FLEV(NAL)-CG)*RO(NAL)/2.0
      SIGYYT(N)=SIGYYT(N)+(SIGYY(N)+Y)*TMUL
      SIGXXT(N)=SIGXXT(N)+(SIGXX(N)+X)*TMUL
      SIGXYT(N)=SIGXYT(N)+(SIGXY(N)+XY)*TMUL
      SIGXX(N)=X
      SIGYY(N)=Y
      SIGXY(N)=XY
      GO TO 321

```

```

328 SIGXXT(N)=SIGXXT(N)+X
   SIGYYT(N)=SIGYYT(N)+Y
   SIGXYT(N)=SIGXYT(N)+XY
321 C=(X+Y)/2.0
   R=SQRTF(((Y-X)/2.0)**2+XY**2)
   XMAX=C+R
   XMIN=C-R
   TMAX=(XMAX-XMIN)/2.0
   IF (Y-X) 325,326,325
325 PA=0.5*57.29578*ATANF ( 2.* XY/(Y-X))
   GO TO 327
326 PA=90.0
327 IF (2.*X-XMAX-XMIN) 405,420,420
405 IF (PA) 410,420,415
410 PA=PA+90.0
   GO TO 420
415 PA=PA-90.0
420 L=N-NBLOCK
421 PRINT 28,(L,X,Y,XY,XMAX,XMIN,TMAX,PA)
C
   IF (NCHECK) 431,431,243
431 PRINT 32
   NFST=NBLOCK+1
   DO 425 N=NFST,NUMFL
   L=N-NBLOCK
425 PRINT 28, L,SIGXXT(N),SIGYYT(N),SIGXYT(N)
C
C   LOADS SET TO ZERO
C
   DO 435 I=1,NUMNP
   M=MNP(I)
   XLOAD(M)=0.0
   YLOAD(M)=0.0
   FRX(M)=0.0
   FRY(M)=0.0
435 CONTINUE
   N=MNP(NUMNP+1)
   NP(N,1)=0
   IF (NAL -NTO) 440,500,440
C
C   MODIFICATION OF LOAD DUE TO REMOVAL OF MATERIAL
C
500 NN=0
   IF (NNN-1) 505,580,502
502 NNN=0
   NID=0
   DO 503 I=1,NFROM
   DSY(I)=0.0
503 DSX(I)=0.0
   GO TO 440
505 PRINT 34, NAL
   PRINT 35
510 NN=NN+1
   LL=NELOUT(NN)
   ET(LL)=0.0
   NFST=LL
   NLST=LL
   M=NTO
   GO TO 181

```

```

520 DL=AREA*RO(NT0)/3.0
    SIG(1)=SIGXXT(LL)
    SIG(2)=SIGYYT(LL)
    SIG(3)=SIGXYT(LL)
    LM(1)=NPI(LL)
    LM(2)=NPJ(LL)
    LM(3)=NPK(LL)
DO 530 JJ=1,3
    M=LM(JJ)
    FRY(M)=FRY(M)+DL
DO 530 II=1,3
    FRX(M)=A(II,2*JJ-1)*SIG(II)/2.0+FRX(M)
    FRY(M)=A(II,2*JJ)*SIG(II)/2.0+FRY(M)
530 CONTINUE
    IF (NN-NOUT) 510,540,540
540 DO 570 M=1,NFREE
    N=NPFREE(M)
    XLOAD(N)=FRX(N)
    YLOAD(N)=FRY(N)
570 PRINT 14, N,XLOAD(N),YLOAD(N)
    NNN=1
    NID=1
    GO TO 129

```

```

C
C   REPLACING MATERIAL
C

```

```

580 DO 590 N=1,NOUT
    L=NELOUT(N)
590 ET(L)=ETORG
    RORG=ROR
    PRINT 34,NAL
    PRINT 36,RORG,ETORG
    NID=2
    NNN=NNN+1
    NFEL=1
    NLEL=NOUT
    GO TO 147

```

```

C
440 IF (NANAL-NAL) 442,442,120
442 CALL EXIT
    END

```